Development of an automated platform for monitoring microfluidic reactors through multi-reactor integration and online (chip-)LC/MS-detection

Hannes Westphal,[a†] Simon Schmidt,[b†] Sanjay Lama,[a] Matthias Polack,[a] Chris Weise,[a] Toni Oestereich,[a] Rico Warias,[a] Tanja Gulder,*[b,c,d] Detlev Belder*[a]

[a]Leipzig University, Institute of Analytical Chemistry, Linnéstraße 3, 04103, Germany
E-mail: belder@uni-leipzig.de
[b]Leipzig University, Institute of Organic Chemistry, Johannisallee 29, 04103, Germany
E-mail: tanja.gulder@uni-leipzig.de
[c]T. Gulder, Organic Chemistry I, Saarland University, 66123 Saarbruecken, Germany
[d]T. Gulder, Synthesis of Natural-Product Derived Drugs, Helmholtz Institute for Pharmaceutical Research Saarland (HIPS) Helmholtz Centre for Infection Research (HZI), 66123 Saarbrücken, Germany

† These authors contributed equally to this manuscript.

Abstract: This work presents a novel microfluidic screening setup with real-time analytics for investigating reactions with immobilised biocatalysts. The setup combines microreactor technology, multi-reactor integration, and online (chip-)LC/MS analysis in a sequential automated workflow. We utilized in-house manufactured fused-silica glass chips as reusable packed-bed microreactors interconnected as individual tube reactors. The potential of this setup was showcased by conducting and optimising a biocatalytic aromatic bromination reaction as the first proof of concept using immobilised vanadium-dependent haloperoxidase from *Curvularia inaequalis* (*Ci*VHPO). The fusion of a HaloTag™ to *Ci*VHPO was used for efficient and mild covalent linkage of the enzyme onto chloroalkane-functionalized particles. Then, the biotransformation was continuously monitored with automated LC/MS data acquisition in a data-rich manner. By further developing the automation principle, it was possible to sequentially screen multiple different connected packed-bed microreactors for reaction optimization while using only miniature amounts of reactants and biocatalyst. Finally, we present a fast and modular chipHPLC solution for online analysis to reduce the overall solvent consumption by over 80%. We established a modern microfluidic platform for real-time reaction monitoring and evaluation of biocatalytic reactions through automation of the reactant feed integration, flexible microreactor selection, and online LC/MS analysis.

Abbreviations

The following abbreviations were used: EtOH = ethanol, MES = 2-(N-morpholino)-ethanesulfonic acid, MCD = monochlorodimedone, IMAC = immobilised-metal affinity chromatography, IPTG = isopropyl-β-d-1-thiogalactopyranoside, Tris = tris(hydroxymethyl)aminomethane, LB = lysogeny broth, NaCl = sodium chloride, NaOAc = sodium acetate, PMSF = phenylmethyl-sulfonyl fluoride, rt = room temperature, SDS-PAGE = sodium dodecyl sulfate polyacrylamide gel electrophoresis.

Other technical and setup abbreviations used are: A/D = analogous/digital, CAD = computer-aided-design, CAM = computer-aided-manufacturing, ESI = electrospray ionization, FS = fused-silica, HPLC = High-performance liquid chromatography, ID = inner diameter, MS = mass spectrometry, OD = outer diameter, PEEK = polyether ether ketone, SLE = selective laser-induced etching.

1. Layouts, fabrication, and modification of microchips and µreactors

The subsequent chapter provides an overview of the different individual microchips used either as µreactors or for chip-based separations. The chips are presented in terms of their design, spatial dimensions, overall functionalities, manufacturing methods and respective preparation steps.

1.1. Microreactor chip - bonded fused silica reaction-chip

For the packed-bed µreactors we used fused-silica glass chips, which were manufactured by an in-house process using a selective laser-induced etching method (SLE), as described in detail in the next section. These chips can be used as efficient and low-consumption reaction vessels for the evaluation of solid catalytic material, such as on particle immobilised enzymes. The benefit of this chip-approach lies in the comparable uniform reactor channel volumes, which, in combination with the integrated µfrit, ensures a reproducible volume of the packed-bed reactor. Each reactor channel can be individually packed, without the need for additional preparational tasks, while providing uniform packed-bed reactors. This feature proves particularly beneficial when comparing several different heterogeneously catalysed flow reactions with each other. It facilitates the testing of different reaction parameters or comparing multiple adjacent reactor channels, each packed with different particulate material (such as different immobilised catalysts or variations in solid support or linker).

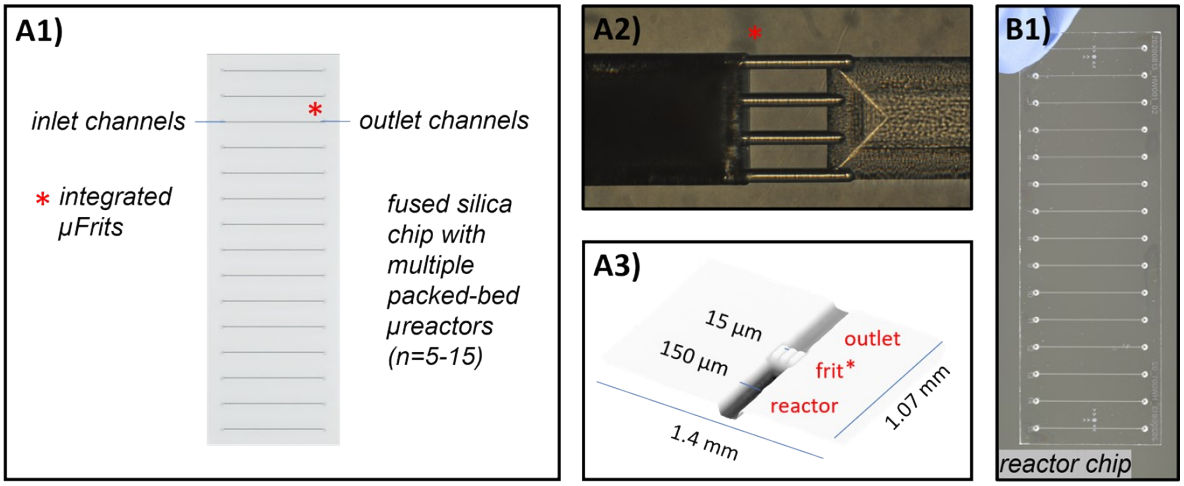

Fig. S1 A1) Schematic representation of the fused-silica chip-based µreactors. A packed-bed column of immobilized catalytic material can be introduced through column packing into the individual µreactor channels. Each channel can be individually packed with different particulate material. **A2)** Microscopic image of the integrated µFrit, which serves as a particle retaining structure during the packing process. The µreactor is filled with particulate material from the left side. **A3)** Laser scanning microscopic image depicting the integrated µFrit and interconnected channels, illustrating their respective spatial dimensions. The small channels of the µfrit are each measuring 150 µm in length and 15-20 µm in width and depth. This measurement was captured from the wafer surface after SLE-structuring and subsequent wet etching but before fusion-bonding with the second top glass slide. **B1)** Photograph of a fully manufactured glass chip, including multiple adjacent reactor channels (outer dimensions of the chip: 76 x 26 x 2 mm). The chip, as shown here, was manufactured from two glass slides as substrates (the detailed manufacturing process is explained in the following section).

The chip design consists of multiple adjacent reactor-channels as shown in Fig. S1 A1 (dimensions for each semicircular reactor channel: 19 mm length, 150 µm width and 65 µm depth, resulting in an approximate empty reactor volume of 265 nl). Each reactor channel terminates in an integrated µFrit which serves as a particle retaining structure for packing the reactor with particulate material (Fig. S1 A2). These µFrits, which operate based on the keystone effect, were directly manufactured during the SLE process (similar to the method described in [1]). The dimensions of the channels and µFrits were measured with a laser-scanning microscope as shown in Fig. S1 A3 (with the kind assistance of Dr. Daniel Splith from the Grundmann group, Leipzig University). The µfrit consists of four small channels, each measuring 150 µm in length, 15-20 µm in width and depth. Behind the µfrit, there

is a short channel (0.9 mm in length, 150 µm in width, and 45 µm in depth), that leads to an outlet hole. Likewise, an inlet hole is present before the reactor channel. Both inlets are connected using in-house manufactured steel clamps for direct capillary connections, typically using either PEEK or FS capillaries (mostly with OD = 360 µm and ID = 50-100 µm).[2] For reactor recycling, the chip can be flushed from the opposite direction with elevated flow and pressure to release the packed material. The chip has mostly been operated with a reactor pump flow rate of 0.2 µl/min at low pressures of 1-5 bar, resulting in an estimated residence time of approx. 40 s for the 19 mm packed-bed reactor (assuming an exclusion volume of 50% for the packed reactor). However, the chip capable of withstanding significantly higher pressures, as demonstrated during reactor packing in the next sections.

- *Manufacturing – microreactor – bonded fused silica reaction-chip*

The µreactor-chips were manufactured by a selective laser-induced etching (SLE) process, followed by wet etching, wafer-to-wafer alignment, glass-glass direct bonding and high-temperature fusion bonding of two fused-silica glass wafers (similar to the method presented in [1]; all SLE processes done by Matthias Polack, Leipzig University). The detailed manufacturing method is explained below. Initially, the chips were designed using the CAD (computer-aided-design) software Autodesk Inventor (Professional 2019; San Rafael, CA, USA) and then processed to the corresponding toolpath and converted to machine code using the CAM (computer-aided-manufacturing) software Alphacam for SLE structuring (CAM designs shown in Fig. S2; Alphacam 2017 R2, Vero Software GmbH, Neu-Isenburg, DE).

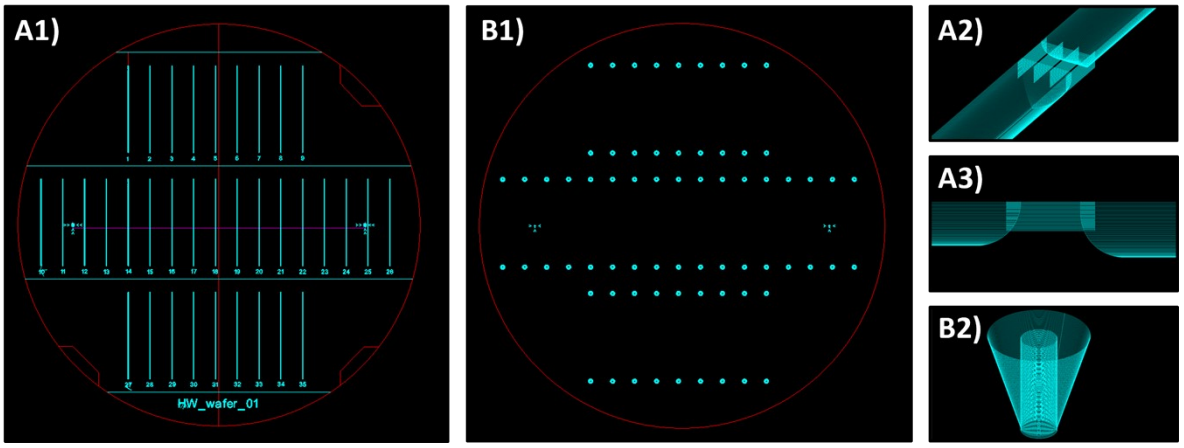

Fig. S2 Visualization of the wafer mask designed for SLE structuring (as processed with the CAM software Alphacam). The laser toolpaths of the integrated features, including outlet holes, channels and the integrated µFrit, are shown on the right. **A1)** Mask for the bottom wafer with integrated channels, **A2)** Magnified top view of the integrated µFrit as particle retaining structure; **A3)** Magnified side view of the integrated µFrit; **B1)** Mask for the top wafer used as a lid with in- and outlet ports for world-to-chip connections; **B2)** Magnified laser path for the outlet holes of the top wafer.

During the SLE process, two 4-inch fused-silica glass wafer (each 1 mm thick) were structured by an ultrashort pulse laser, which transferred the design into the glass substrate (Fig. S3 A1; 1030 nm ± 5 nm Yb:YAG laser; pulse energy: 230 nJ, pulse length: 400 fs; FEMTOprint f200 aHead P^2, Muzzano, CHE). For the laser-treated areas the glass etching rate is significantly increased, allowing selective wet etching of the structured design by applying KOH solution in an ultrasonic bath (8 M, heated to 85 °C, 6 h). Two wafers were individually structured for the respective chip design. One wafer contained the semicircular reactor channels and µFrits, while the other wafer included the outlet holes for world-to-chip connections (as shown in Fig. S3 A2-3).

After processing and etching, both glass wafers were cleaned with DI-water (water filtered through 0.2 µm; Smart2Pure, TKA Wasseraufbereitungs GmbH, Niederelbert, DE) in multiple washing steps, using water and piranha solution (water filtered through 0.2 µm; Smart2Pure, TKA Wasseraufbereitungs GmbH, Niederelbert, DE). Subsequently, the wafers were placed in a wafer aligner (Fig. S3 B1; AWB-04 Aligner Wafer Bonder, Applied Microengineering Ltd (AML), Oxfordshire, UK) to align the channels

and inlet holes. Before to the camera-aided alignment, the substrates were cleaned using an oxygen plasma (500 V, 100 mA). The chamber was then evacuated, water vapour was injected, the substrates were aligned and put together, using a force of 1 kN and 200 °C for 3 h, resulting in a slight pre-bonding of the two aligned wafers (Fig. S3 B2).

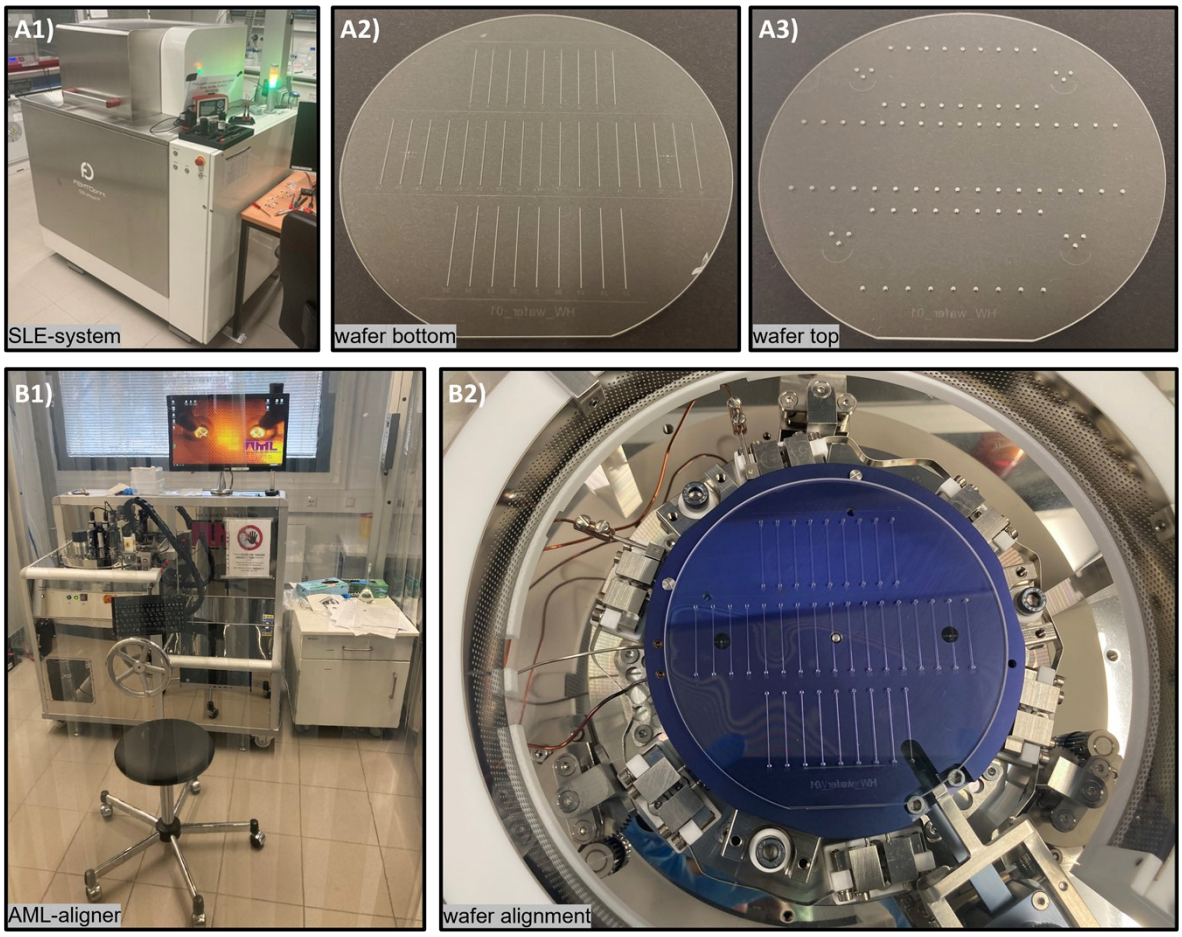

Fig. S3 Laser-structuring and alignment of the two processed wafers. **A1)** Device for SLE-processing of the designed masks (f200 aHead P^2, FEMTOprint SA, Muzzano, CH); **A2)** Processed and etched unbonded bottom wafer with the respective integrated channels and µFrits. **A3)** Processed top wafer used as a lid with in- and outlet ports for world-to-chip connections; **B1)** Wafer aligner for optimal camera-aided positioning of the two processed wafers (Aligner Wafer Bonder, Applied Microengineering Ltd (AML), Oxfordshire, UK); **B2)** Pre-aligned wafer inside of the chamber of the wafer aligner prior to high-temperature fusion-bonding.

The substrates were then fusion-bonded using a high-temperature bonding programme (Fig. S4 A1; approx. 53 h, up to 1050 °C; furnace L 5/13 P330, Nabertherm, Bremen, DEU). The bonded substrate was evaluated and based on the success of the bonding (determined by the observation of the total fraction of bonded area), several rectangular chips were diced, each containing a varying amount of µreactors. Dicing of the chips was performed using a water-cooled diamond-blade saw (Fig. S4 B1-3, with the kind assistance of Monika Hahn from the Grundmann group, Leipzig University; Saw Model 15, Logitech Limited, Glasgow, UK).

Alternatively, similar chips were manufactured using two rectangular glass slides as bonding substrates instead. These slides were etched out of the wafer already during the SLE process when the channel design was structured (as shown in Fig. S4 C1-2; outer dimensions of the chip: 76 x 26 x 2 mm). This approach did not require a separate dicing step and resulted in high-quality (produced by Matthias Polack, Leipzig University). However, it was a more challenging manufacturing process due to inconsistent bonding results. The other manufacturing steps for this approach were similar to the previously discussed method, involving the alignment of the processed glass-slides (AML) and subsequent high-temperature fusion-bonding.

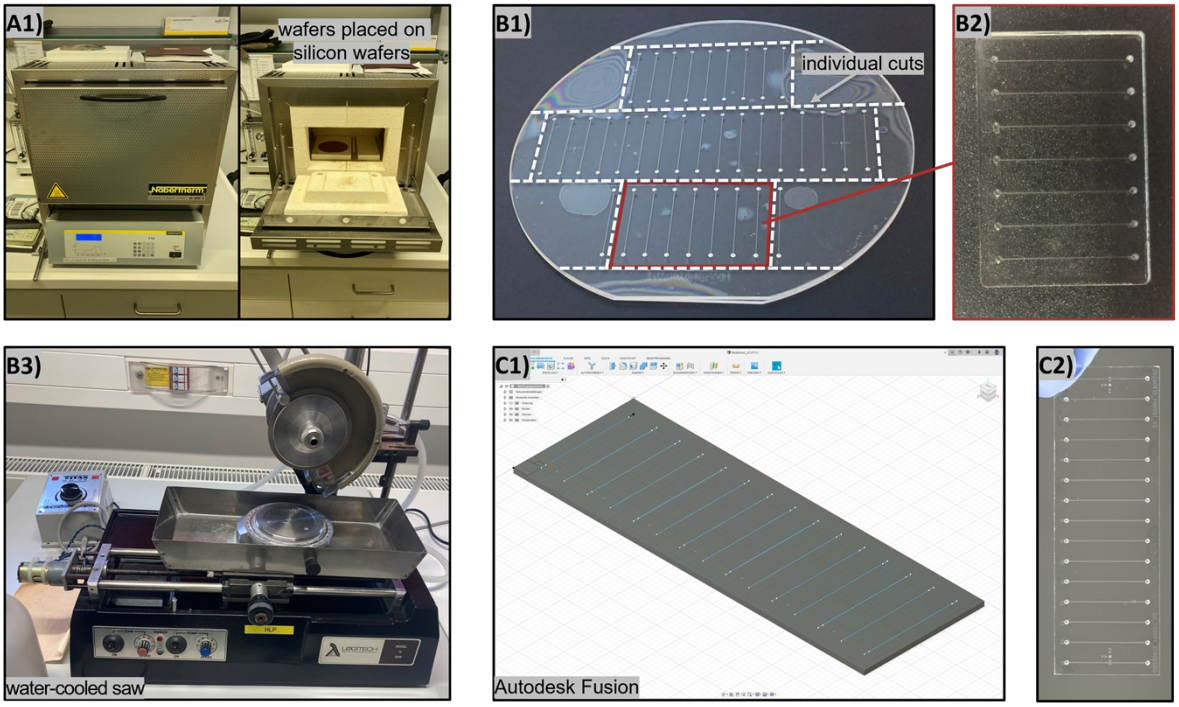

Fig. S4 Fusion-bonding and wafer dicing as final chip manufacturing steps. **A1)** Furnace used for fusion-bonding of the pre-aligned wafer-substrates (heating up to 1050 °C; L 5/13 P330 muffle furnace, Nabertherm, Bremen, DE); **B1)** Fusion-bonded glass substrate (lighter areas, or Newton rings, indicate insufficient bonded areas). The white dashed lines indicate the cuts made in the subsequent dicing process to obtain rectangular chips; **B2)** Final diced chip from the bonded wafer substrate; **B3)** Water-cooled diamond-blade saw used for wafer dicing (with the kind assistance of Monika Hahn from the Grundmann group, Leipzig University; Saw Model 15, Logitech Limited, Glasgow, UK); **C1)** Alternative design using rectangular substrates already etched from of the wafer during SLE-manufacturing. No further dicing was necessary for this design. **C2)** Photo of the final bonded chip using the alternative method without further dicing.

- *Preparation/Modification – microreactor – bonded fused-silica reaction-chip*

Slurry-packing: The packed-bed µreactors were packed using a slurry-packing technique after manufacturing. Due to the integrated µFrits (Fig. S1 A2/A3), the µreactor channels could be easily packed by connecting the µreactor channel inlet to an HPLC-pump and a 6-port valve with a sample loop (volume approx. 100 µl). The sample loop was filled with a suspension of the particulate material (approx. 2-5 mg/ml). By switching the valve position, the particles could be packed directly into the reactor channel using flow rates ranging from approx. 3-30 µl/min and a pressure of up to a maximum of 60-100 bar. The entire reactor volume was packed till the inlet hole, ensuring to provide a reproducible packing volume (1.9 mm length). To prevent particle sedimentation, the chip and the sample loop were placed in an ultrasonic bath (Sonorex, Bandelin) during the packing process.

Reactor recycling: The µFrit, as shown in Fig. S1 A2/A3, is positioned only on one side of the reactor channel, allowing for easy reuse of the chip. This could be achieved by connecting a pump to the opposite inlet, and the particulate material was flushed out using an elevated flow rate and applied pressure (typically at pressures around 100 bar). Placing the chip in an ultrasonic bath helped to loosen up the packed column, facilitating the µreactor recycling process.

1.2. ChipHPLC - bonded borosilicate glass chip

For chip-based separations, as later integrated into the setup, mostly bonded borosilicate glass HPLC-chips were used as shown in Fig. S5, which have already been presented in several publications of the

group ([2–6], as well as in a recently published collaborative project [7]). The chips can be used for efficient and low eluent and sample consumption, fast and high-pressure chromatographic separations, while running at low to mid eluent pump flow rates (in the literature used between 10−1000 µl·min^{-1} for the elution pump, depending on the split ratios, restriction capillaries and pressures utilised (in this study 75-100 µl·min^{-1}). Due to the flow split at the column head, this results in a column flow of 15−1400 nL·min^{-1}.[3,6] Respective van Deemter plots for the linear velocity can also be found in the cited publications.[8]). The HPLC-chips were manufactured by iX-factory (now part of Micronit GmbH, Dortmund, Germany, DE; outer dimensions chip: 45 x 10 x 2.2 mm; semicircular separation channel: 35 mm length, 90 µm max. width, 40 µm depth) and subsequently packed with a chromatographic column using either XBridge (C18, 2.5 µm particles, Waters) or Poroshell (C18, 2.7 µm particles, Agilent) as particulate column material. Before packing, photopolymerized frits were integrated, as particle retaining structures. The chip column was then slurry-packed through a packing channel, which was sealed past packing by integrating a photopolymerized plug at the cross section to the column channel. In addition, the chip design consists of an integrated injection cross, which allows the direct injection of a low-dispersed sample plug onto the packed separation channel (instrumental setup shown in section S2.2 and injection principle and valving explained in detail in section S5.3). Beyond the separation column, the chip was grinded to form a pyramidal monolithic electrospray-emitter, which was then silanised, for direct MS-hyphenation. During operation the chip was grounded via fluidic contact to the connected HPLC-pumps.

The initial chip design included an additional sheath flow channel after the separation column, which could be used to add an aqueous fraction to maintain stable electrospray generation if for example normal phase separations would be conducted. However, this sheath channel, as well as an additional outlet channel after the separation column, were both grinded off during emitter preparation as they were not used in this application. One original design variation also included integrated sputtered electrodes for applying external voltage, which could be used for applications where the MS-inlet is connected to ground, which was not used in this project (since for the utilized Bruker AmaZon SL instrument, the high-voltage is applied at the MS-inlet).

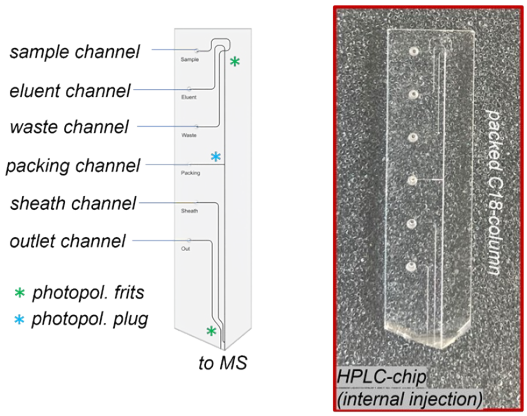

Fig. S5 A) Schematic sketch of the used HPLC-chip, as developed by our group ([2–6], as well as in a recently published collaborative project [7]). The sketch illustrates all fluidic inlet channels, as well as the positions of the photopolymerized frits (as particle retaining structures for the packed column), and plug (used to seal off the packing channel past column integration). The respective instrumental setup is shown in section S2.2 and the injection principle and valving explained in section S5.3. **B)** Photo of a fully prepared HPLC-Chip (outer dimensions: 45 x 10 x 2.2 mm)

- *Manufacturing – chipHPLC – bonded borosilicate glass chip*

The borosilicate HPLC-chips were manufactured by iX-factory (now part of Micronit GmbH, Dortmund, Germany, DE) using an in-house process, after the respective chip design was provided (process details also described elsewhere[2,3,5,9]). In summary, the process involved the fabrication of chips from Borofloat-33 glass substrates by using photolithography, wet-etching with hydrofluoric acid (HF) and subsequent high-temperature fusion bonding. Further information on the manufacturing process can be withdrawn elsewhere.[9]

- *Preparation/Modification – chipHPLC – bonded borosilicate glass chip*

Detailed information on the preparation steps as well as the compositions of the polymerization mixtures can be found elsewhere and is therefore only briefly described here.[10–12]

Photopolymerized frits: At both ends of the separation channel of the chipHPLC photopolymerized frits were integrated as particle retaining elements before packing (in contrast to the on-chip integrated µFrits of the previously presented µreactor chips). These frits were integrated by first introducing a polymerisation mixture by a syringe through one of the chip-inlets, which was then locally irradiated by using a focused 365 nm LED.

Column packing: The column was then slurry-packed with the particulate column material through an additional packing channel, while the general procedure being similar to that described in packed-bed µreactor chip preparation from section S1.1. Compared to the µreactor channels, increased flow and pressure were used for packing the separation column and the separation column was sealed after packing. Furthermore, the packing procedure was adapted to the different particle retaining structure and the chip was connected through an additional packing channel instead. The particles were then packed onto the photopolymerized frits at the ends of the separation channel using a flow rate of approx. 3 to 20 µl/min (pressures around 100-250 bar, depending on particle size etc.). For the chips used in this publication C18-particles were used as particulate column material (XBridge, 2.5 µm, Waters).

Photopolymerized plugs: The separation channel was sealed past packing by the integrating a photopolymerized plug directly at the end of the packing channel. In general, this process was similar to the photopolymerization of the porous frits, using the same 365 nm LED. However, an HPLC-pump (LC-20AD, Shimadzu, Kyoto, JP) and an additional sample loop valve were used to introduce the prepolymer solution onto the column.

Integration ESI-emitter & silanisation: Grinding the chip past the separation column to a pyramidal monolithic electrospray emitter. Afterward the emitter was hydrophobized using an in-house protocol. For that purpose, the emitter was first put in contact with 1 M NaOH (30 min), then with water (flushed), anhydrous iPrOH (flushed; dried via molecular sieve, 3 Å pore size) and anhydrous isooctance (flushed; dried via molecular sieve, 3 Å pore size). Thereafter, the emitter was silanised with 10 vol% trichloro(1H,1H,2H,2H-perfluorooctyl) silane in anhydrous isooctane (10 min). At the end, the residual reagent was removed again with anhydrous isooctane (flushed). During the whole process, a slow solvent stream was pumped along the chipHPLC column to avoid either silanisation of the column or clogging of the emitter channel (2-5 µl/min ACN).

1.3. ChipLC – simple bonded soda-lime glass Chip

During the development of the chip-based separation setup, a lower flow-rate version of the chipHPLC was also tested, along with a comparably lower operational pressure. For this purpose, a bonded soda-lime glass chip was utilised, as shown in Fig. S6. In contrast to the previously introduced borosilicate chipHPLC, this chip had a simpler design lacking and was without an internal injection cross. Consequently, an additional an additional injection valve was required for sample injection (5 nl; Nanovolume valve, Cheminert, Vici Valco). The setup and evaluation of this system are described in detail in section S5.3. In this configuration, a full flow approach was used, thus no flow splitting was used before the column (as for the other chipHPLC). The chip was operated with an eluent flow rate ranging from 0.75-1.00 µl/min (tested for different compositions of ACN:H_2O, at pressures around >40 bar), which was similarly low as the consumption range of the coupled µreactor chip (using mostly 0.2 µl/min, with 2 µl/min dilution). As will be demonstrated later, the separation of the reaction compounds was generally possible with this chip design. However, in terms of performance, the previously presented chipHPLC was preferable (section S1.2, flow range 75-100 µl/min).

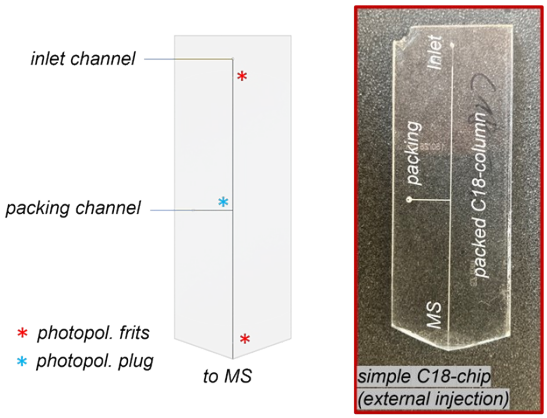

Fig. S6 A) Schematic sketch of the simpler low-flow chipLC variant as an alternative to the previously presented chip-HPLC of section S1.2. Detailed evaluation of this chipLC variant can be found in section S5.3. **B)** Photograph of the manufactured and packed chipLC for testing lower operational flow rates.

- *Manufacturing – chipLC – simple bonded soda-lime glass Chip*

The bonded soda-lime LC-chip (full-flow approach with external injection) was manufactured by an in-house rapid prototyping process using photolithography, wet-etching and subsequent high-temperature fusion bonding of two soda-lime glass slides (each approx. 76 x 26 x 1 mm). Detailed information on the fabrication process of the soda-lime glass chips can be found elsewhere and is thus not described in detail here (for both publications referred detailed information is provided in the respective ESI).[11,12]

- *Preparation/Modification – chipLC – simple bonded soda-lime glass Chip*

Like the previously described borosilicate HPLC-chip, the particulate column material was introduced by slurry-packing through an additional packing channel on photopolymerized frits as particle retaining elements (column particle: Exsil Pure C18MS, 3 µm, Dr Maisch GmbH, DE). The packing channel was also similarly sealed by a photopolymerized plug and a pyramidal ESI-emitter was grinded for MS-hyphenation. More detailed information of the preparation steps can be found in the previous section of the HPLC-chip or elsewhere (for both publications referred, detailed information is provided in the respective supporting information).[11,12]

2. Instrumental setup

In the following abstract, the instrumental setup is illustrated and described in detail. First, the overall instrumentation and flow circuits are depicted, along with an explanation of the injection principles. Afterward, the general principle for setup automation is presented, as well as the structure of method sequencing for multi-reactor operation with semi-continuous online LC/MS analysis of the reactor effluent. In short, the automation method enables running either long-term measurements of individual continuous µreactors or performing sequential multi-reactor monitoring, also with sample variation.

Furthermore, an alternative variation of the online analytical part of the setup presented in this section. This variation involves replacing the conventional HPLC/MS with a low consumption chip-HPLC/MS. This setup variant not only reduces the overall eluent solvent flow (to a range of 75-100 µl/min), but also enables fast separations using an on-chip injection method, which is briefly introduced. Afterward, another chip variant, featuring an even lower flow rate and external injection principle, is briefly introduced. This variant is also discussed and compared to the other approaches presented.

2.1. Setup – µreactor-LC/MS – Valving, instrumental and general operation principles

The complete instrumental setup for integrating the previously presented µreactors into a conventional online LC/MS analysis is depicted in Fig. S7. A brief description of all instrumental components, including pumps, capillaries, connections, valves, and electronic components is provided below. The setup can be divided into two different sections: one for µreactor operation and one for online analysis. The first section enables the connection and selection of either one or multiple µreactors (details about used µreactors can be found in the previous section S1.1). The second section is used for the subsequent online LC/MS-analysis, which can be performed using either a conventional column or a chipHPLC approach (detailed information about the respective chips can be found in section S1.2).

The system is operated by using three HPLC pumps. The first pump controls the continuous flow through the µreactor (typically at 0.2 µl/min, MES buffer pH 6.0; LC-20AD, Shimadzu). The second pump provided the sample dilution past the reactors (mostly 2 µl/min, 40:60 ACN:H_2O, v/v; 1260 Infinity isocratic HPLC pump, Agilent, Santa Clara, US). The third pump was utilized as the LC-eluent pump (600 µl/min, 70:30 ACN:H_2O, v/v, 0.1 % FA; 1260 Infinity binary HPLC pump, Agilent), directly flowing onto the subsequent HPLC-column (Zorbax Eclipse Plus C18, 4.6x100 mm, 3.5 µm, Agilent). In one variation of the setup, no dilution of the reactor effluent was used. Instead, a smaller sample loop was integrated for online analysis sampling (0.2 µl loop instead of 2 µl).

All connections in the setup were made using commercially available PEEK and FS capillary tubing (50 and 100 µm ID, 360 µm or 1/16“ OD) and PEEK connections such as screws, ferrules, crosses, plugs, and other fittings (primarily Nanovolume fittings for 360 µm OD, Cheminert, VICI AG). Inline filters (2 µm, SS frit, JR-0611-SS2-3, VICI AG International, CHE) were added after the pump outlets and sample syringes to prevent particle contamination. To connect the chips with the outer periphery, a homemade steel clamp system was utilised.[2] The main fluidic circuit was realized by four electrically actuated Nanovolume valves, which were mounted on a custom-built metal platform for stability. Several two-position valves and selector valves were used, the individual functions of which are described below (100 µm bore, 360 µm fitting connections, 10-port versions, C72MPKH-4670ED & C5M-4300EMH, Cheminert, VICI AG, Schenkon, CH).

The first valve contains a large sample loop as reaction mixture reservoir for providing a constant sample feed onto the subsequent µreactors over multiple hours (e.g., 300-1000 µl, using PEEK capillaries with IDs of up to 750 µm). In position A, the sample loop can be loaded with the respective reaction mixture by using a glass syringe (Hamilton, Bonaduz, CH). By switching the valves to position B, the reactants can be flushed toward subsequent reactor positions for continuous operation. As an alternative to the first sampling valve, an autosampler was integrated during later measurements, enabling sample variation during single pre-sequenced runs for multiple reactor evaluation (40 µl autosampler injection loop; G1377A Micro WPS, Agilent).

The second and third valves are selector valves, which allow for the individual selection of µreactor at ten different positions. These valves are connected before and after the µreactor channel, and by switching both selector valves simultaneously to the same position, a specific reactor can be chosen (as both the reactor in- and outlet). Detailed examples of using different reactor positions in single sequenced experimental runs are described in section S5.2.

The fourth valve is part of the subsequent analytical setup and enables sequential sampling of the reactor effluent for online LC/MS analysis. In position A, or eluent mode, the reactor effluent flows through the sample loop and into a waste channel (sample loop size either 0.2 µl or 2 µl, depending on whether a previous flow dilution is used). By switching the valve to position B, or injection mode, the sample loop is loaded onto the HPLC column and eluted by the connected eluent pump. It is important to note that for chipHPLC integration, a different setup variant and injection principle were used, as described in section S2.2.

All valves were externally controlled by a „Colibrick“ A/D converter box in combination with a ”Clarity chromatography data station” (DataApex, Prague, CZ). This allowed for the automation of the injection principle and complex sequencing, as explained in detail in section S3.1. For MS-detection after chromatographic separation, a quadrupole ion trap mass spectrometer was used (detailed information on MS-coupling can be found in section S2.3; AmaZon SL, Bruker Daltonik GmbH, Bremen, DE).

A) instrumental setup - picture

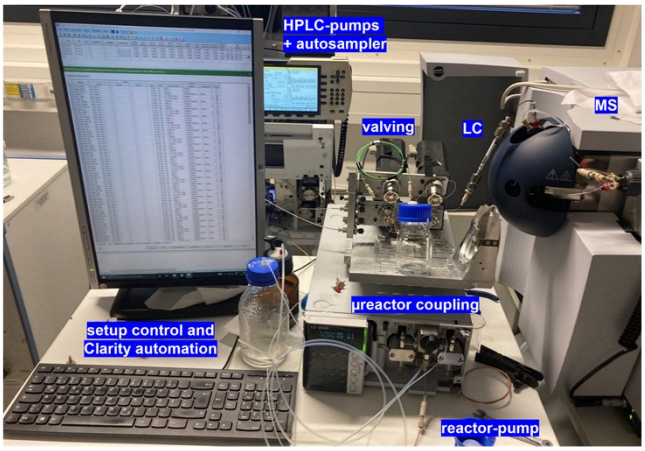

B) instrumental setup - schematic

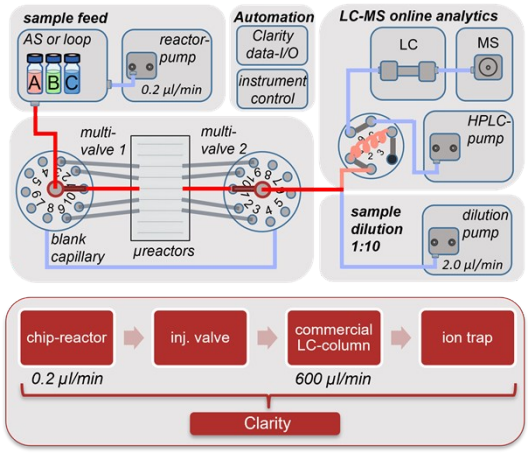

Fig. S7 Overview of the Instrumental setup with LC/MS-detection. **A)** Photograph of the complete instrumental setup. The respective valves and HPLC-pumps and acquisition duty cycle were controlled by Clarity automation as described in detail in section S3; **B)** Schematic sketch of the respective valving, and setup structure, as well as a simplified visualization as a flow chart.

2.2. Setup – µreactor-ChipLC/MS

As mentioned above, the instrumental setup can be divided into two distinct sections. The first section for µreactor operation and the second one for the online LC/MS analysis. These sections differ significantly in terms of flow rates and solvent consumption. To address this, an alternative variant to the conventional HPLC-column was developed by integrating a chip-based chromatography unit. This section focuses on the instrumental setup and the on-chip pinched-injection principle, building upon the previously introduced chipHPLC. The detailed fluidic setup for chipHPLC integration is depicted in Fig. S8 and can be seamlessly incorporated into the analytical LC/MS-part of the previously shown setup in Fig. S7. The chipHPLC setup is relatively compact (as shown in Fig. S8 A-B), consisting of a single HPLC pump (the general chipHPLC-setup was based on a recent joint publication[7]), a 10-port Nanovolume valve (100 µm bore, Cheminert, VICI AG, Schenkon, Switzerland), an external pressure sensor (Duratec Analysentechnik GmbH, Hockenheim, Germany), and commercially available high-pressure PEEK fittings and connections (mostly OD 360 µm PEEK capillaries with varying inner

dimensions, VICI). The sample feed can either be provided by the constant effluent of the reactor setup, as presented before, or during testing, it can be provided externally using a syringe. A detailed description of the injection principle can be found in section S5.3. Similar to the rest of the setup, the valve is externally controlled to automate the duty cycle of the chipHPLC injection principle (general automation principle explained in section S3.1). All capillary lengths and diameters of the setup are listed below in Fig. S8 C.

A) chipHPLC - isolated

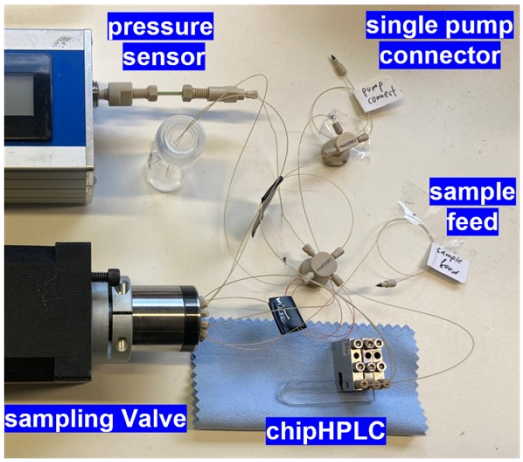

B) chipHPLC - integrated

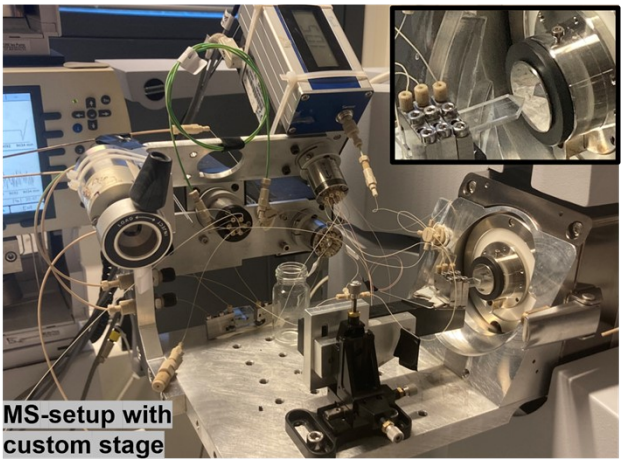

C) chipHPLC – valving and tubing diameters

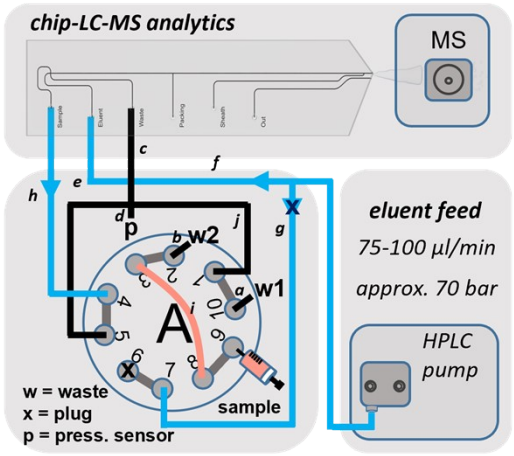

Label	Description	PEEK capillary dimensions
a	waste 1 restriction	360 µm, 25 µm, 22 cm
b	waste 2 restriction	360 µm, 100 µm, 20 cm
c	chip to waste 1	360 µm, 75 µm, 15 cm
d	pressor Sensor	360 µm, 100 µm, 10 cm
e	valve to waste	360 µm, 75 µm, 15 cm
f	flow split to chip eluent	360 µm, 75 µm, 20 cm
g	flow split to valve	360 µm, 100 µm, 20 cm
h	valve to chip sample	360 µm, 75 µm, 15 cm
i	sample loop, 5 µL	360 µm, 125 µm, 40 cm
J	valve to cross	360 µm, 100 µm, 20 cm

Fig. S8 Instrumental fluidic setup for operating the chipHPLC with integrated injection cross. **A)**. Photograph of the easy to implement chipHPLC setup that utilizes only a single Nanovolume valve, commercial high-pressure PEEK connections (primarily 360 µm connections, VICI), an HPLC eluent pump, and an external pressure sensor The sample feed shown can be directly coupled to the µreactor effluent for online monitoring. The chip is connected to the setup by using in-house built steel clamps. **B)** Photograph of the chipHPLC setup in front of the MS inlet, using a custom metal stage for mounting the chip and the connected valve. The stage was also used for stabilizing the valves of the reactor setup. **C)** *left:* Schematic of the respective valving (principle adapted and modified from a joint publication [7]). *Right:* overview of all capillary lengths and diameters as used in the chipHPLC setup.

2.3. Coupling with mass spectrometry

For MS-detection of both commercial LC and chipHPLC separations, a quadrupole ion trap mass spectrometer (AmaZon SL, Bruker Daltonik GmbH, Bremen, DE) was utilized. For the commercial LC-column (Zorbax Eclipse Plus C18, 4.6x100 mm, 3.5 µm, Agilent) the column was directly connected with a PEEK capillary to the conventional spray chamber and ESI-emitter. During electrospray operation, the

transfer capillary voltage was set to 4500 V, and the offset endplate to 500 V. The mass spectrometer was consistently operated in positive and enhanced resolution mode with a scan range of 50 to 500 m/z at an acquisition rate of approximately 3 spectra·s^{-1} (averages set on 2-5). An additional dry gas flow of 8 L·min^{-1} was maintained at a temperature of 300-340 °C.

When using a chipHPLC as the ESI-emitter, the chip was positioned on a custom metal stage, which could be directly connected to the MS inlet, allowing for stabilization of the connected valves. To achieve precise alignment of the chip emitter in front of the MS inlet, a three-axis miniature linear translational stage (T12XYZ/M and T12B, Thorlabs, New Jersey, USA) was employed. The precise positioning of the chip emitter depended on the flow rate and composition of the mobile phase (typically approx. 2-3 mm). During this operation, the chip was grounded through fluidic contact with the connected HPLC-pumps. Additionally, a lower dry gas flow of 4 L·min^{-1} at a temperature of 225-250 °C was applied.

3. Automation of the injection principles, sequencing, and data evaluation

To control the instrumental setup and automate the injection principle, a ”Clarity chromatography data station” was utilized in combination with a ”Colibrick” A/D converter box (DataApex, Prague, CZ). Even though we presented a similar, principle of automation and instrumental control in previous publications (detailed previous description of the automation principle can be found in the ESI of the references),[11,12] the method has been further developed and optimized specifically for this application. In the following, first all different connections for setup control and signal monitoring are listed. Subsequently, the automation principle for sequential single- or multi-reactor operation and is explained in detail. Finally, a brief description of the Python-based workflow for subsequent data evaluation is provided at the end of the section in S3.2.

3.1. Instrumental setup hardware automation principle

- *Connections for instrumental control and monitoring*

Firstly, all respective connections between the instruments of the setup are shown in Fig. S9. For this purpose, a ”Colibrick” A/D converter box was used, capable of running up to 4 channels for analogue data logging. These channels were used to monitor the pressure of the connected pumps, as well as an external pressure sensor for the chip-based separations (DET). In addition, the ”Colibrick” box also includes 4 digital outputs (TTL, 5 V logic, functioning as relay contacts), which were used as external triggers. Two of these outputs were used to trigger the start/stop of the MS-acquisitions, by addressing the auxiliary I/O-pins of the Bruker AmaZon SL ion trap mass spectrometer (Pin 28: 5 V, Pin 24: start, Pin 25: stop). An additional output was utilized to potentially stop the Shimadzu reactor pump at the end of the run. The other pumps were connected through external LAN cards and controlled using the Agilent ICF library („Instrument Control Framework”) in the ”Clarity” software. This library was also used for controlling the implemented autosampler, enabling different sampling for different reactor positions within a single sequential run. To enable the sequential automation principle, we used the last digital output to trigger the A/D converter box itself. This ensured the automatic initiation of the next entry in the ”Clarity” acquisition sequence table. For that purpose, the digital output was connected to one of the 4 additional digital inputs of the A/D converter box (TTL, 5 V logic; IN 1 as an external start, closed connection, „down“ here as default). The other digital inputs were mainly not used. Finally, the 4 electrically actuated Nanovolume valves were connected through serial-to-USB converter to enable control with the ”Clarity” software as well.

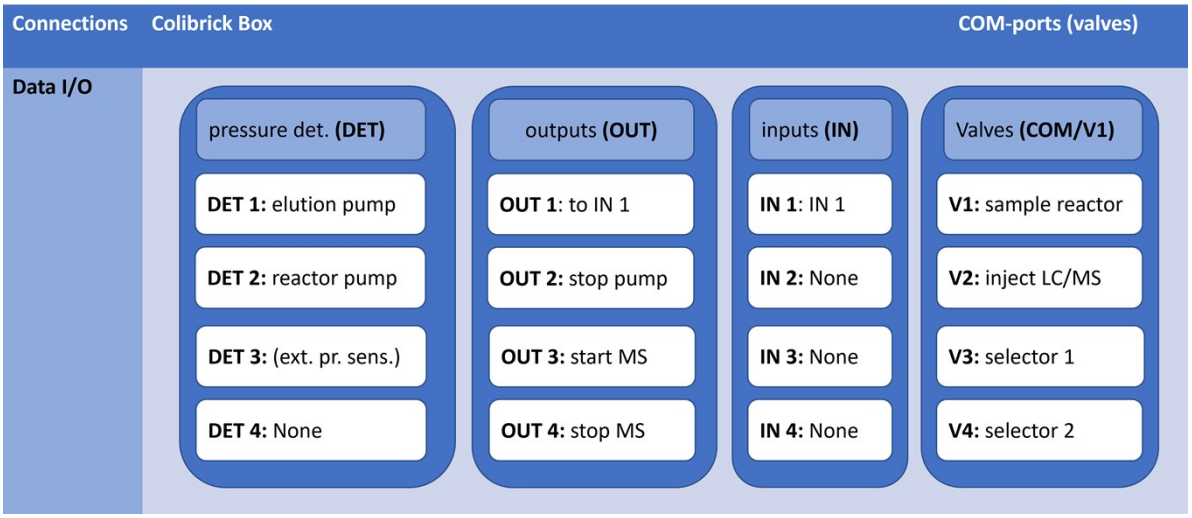

Fig. S9 Illustration featuring the I/O-connections and analogous detection channels for pressure monitoring. For most serial connections a „Colibrick“ A/D converter box was utilized in combination with a ”Clarity” chromatography data station (DataApex, Prague, CZ). The valves were connected via USB and addressed through their respective COM-ports. Additionally, for further pump and autosampler control the Agilent ”ICF”-framework was used within the ”Clarity”-Setup, with the devices connected via external LAN-cards.

- *Sequential automation method for addressing multiple reactors*

In the following section, a detailed description of the sequential automation methods for acquiring long-term measurements is provided. By controlling the pumps, valves and MS-triggering, sequential measurements can be acquired iteratively. Initially, this approach was used for long-term monitoring of single packed-bed µreactors with constant sample feed for testing overall catalyst stability and performance by reaction monitoring of the model biotransformation. For these runs blank measurements were acquired manually either before or after the respective reactor run. Subsequently, the integration of the two ”Nanovolume” selector valves enhanced the setup flexibility by enabling the switching between multiple reactor positions. This facilitated not only the comparison of multiple µreactors packed with different catalytic materials. Finally, by the integration of an autosampler before the µreactor selector valves the flexibility during individual runs could be increased, as multiple different reaction samples could be tested sequentially on similar or different µreactor positions as demonstrated in section S5.2 (variation of the sample feed). It was also possible to switch to a novel µreactor with fresh unused catalyst, after a decrease in catalyst activity was observed. Furthermore, other functionalities such as blank capillaries could be integrated for cross-evaluation. By that, blank measurements could be acquired before or between reactor runs by simply switching to a reactor position with a blank capillary (further discussed below).

For visualisation of the general sequence structure, multiple method blocks are presented schematically in Fig. S10, each including several LC/MS acquisitions and individual functions. The different methods are presented and explained in the following section using a custom naming convention. Then, the underlying functions shortly presented as well.

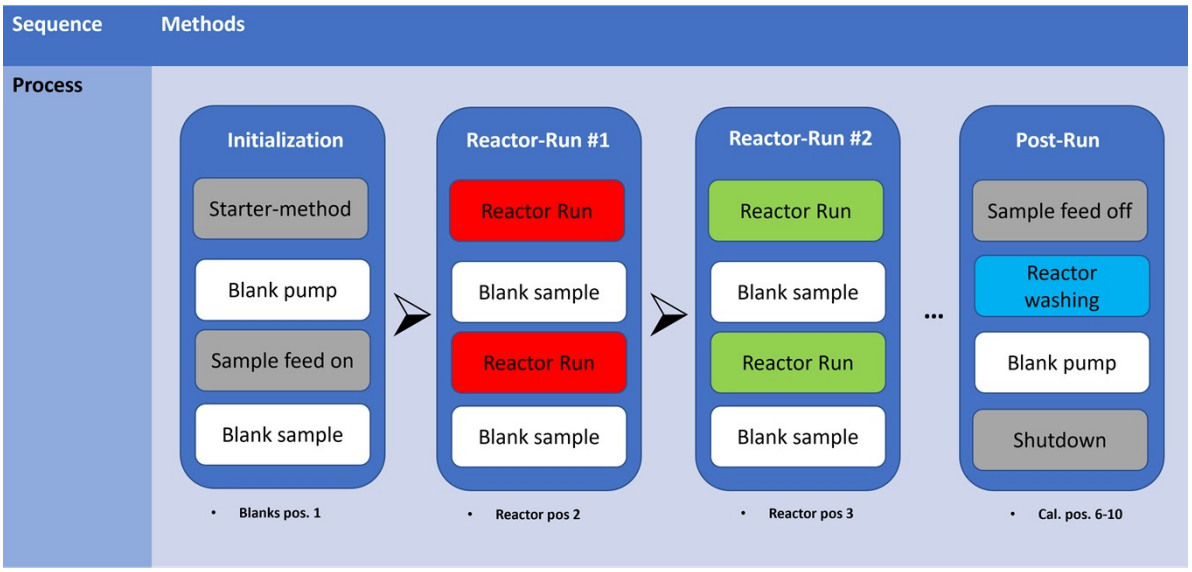

Fig. S10 Visualization of the sequence structure by summarizing methods as method blocks. Here, an exemplary sequence is shown using different blocks for sequentially running two different reactor runs (including multiple reactor runs or blank sub methods as explained in the next section). Initial reactor runs before multi-valve integration were carried out without acquiring blank acquisition in between.

Each run consisted of multiple method blocks, depending on the connected µreactor configuration and planned experiments. Generally, each multi-valve run was started by an initialization, during which respective sequence was started and the selector valves were connected to a blank capillary (pos. 1). Initially, blank acquisitions of the reactor pump stream were measured, followed by the coupling of the sample feed into the system. Subsequently, similar blank measurements of the sample stream were acquired to validate the sample flow toward the reactor positions and through the sample loop of the analytical section. This step ensured that when the selector valves were switched to a different reactor position, the sample feed flowed directly onto the reactor with minimal delay. For each subsequent acquisition the duty cycle involved sampling the reactor flow toward the analytical section and then performing an LC/MS measurement using the respective external valving and MS auxiliary pins for starting the measurement.

The next blocks consisted of reactor runs to investigate the connected packed bed µreactors. Within each block, sample feed blanks were performed in the middle of the run as well as at the end of a reactor run. The purpose of the respective blank measurements is explained below. Then, reactor washing steps were conducted and the system was shut down by stopping all pumps, so that measurements could also be run over night. As mentioned before, each of these discussed methods (from Fig. S10) consisted of further individual functions as subparts (as shown in Fig. S11) and briefly explained below. Each of these functions were constructed using the integrated method event table in the ”Clarity” software, which facilitated an easy and efficient control of the valves and outputs for the desired automised instructions. The individual sequences and event tables for each performed run are shown in detail in section 5.2.

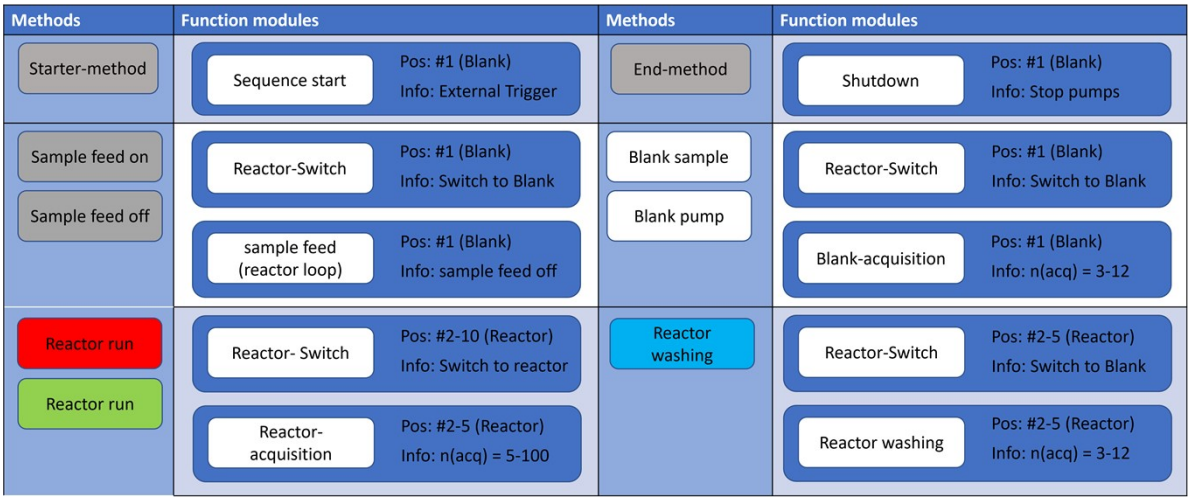

Fig. S11 Describing the respective methods and underlying functions as described in the previous section (or as depicted in Fig. S10). For each function the respective reactor position of the connected selector valves is stated, as well as how often the function is performed iteratively.

Blank pump (pump feed): Blank measurements were conducted at the start of each run by switching the selector valves to a blank PEEK capillary (which was integrated at one of the reactor positions, typically pos. 1). These measurements were acquired before introducing the sample feed, thus only buffer signal from the reactor pump should be visible (as shown in Fig. S12 A). The purpose of these blanks was to evaluate the signal regarding overall signal intensity, stability, and the presence of potential of blockages or contaminants in the fluidic setup (acquired mostly n=1-5 blanks). These measurements are referred to as ”Blank pump” or ”B” in the following.

Blank sample (sample feed): After introducing the reactor sample feed into the fluidic setup, additional blank measurements were conducted, following the same procedure as described before. For that purpose, the selector valves were also positioned to a blank capillary to monitor the now integrated sample feed. Thus, in the LC/MS-analysis only the buffer and the reactant peaks should be visible (as shown in Fig. S12 B). These sample blanks were acquired before, during and in between reactor runs as explained in the following. As the sample feed is not included in these blank measurements, they are referred in the following sequences as ”Blank sample” or ”r”.

Before starting a reactor run, these blanks were monitored to visualise the time it takes for the sample feed to reach the analytical loop. This ensures successful integration of the sample feed through the reactor line, assuring also direct swept volume free coupling when switching to another reactor position. Additionally, these blanks can be used to observe the stability of the sample feed and validate potential product formation in the absence of enzyme addition (e.g., at increased H_2O_2 concentrations for the model biotransformation used). Furthermore, the initial intensity of the reactant signal can be used to directly calculate reactant conversions for subsequent reactor runs.

In the middle of a reactor run, similar blank acquisitions were also measured to observe the consistency of the sample feed and examine the response of the analytical loop for any potential carry-over effects from the reactor (e.g., traces of sticking product). It could be observed that the product signal breaks in as soon as the switch was made from a reactor to a blank capillary position and the reactor line till the analytical loop was flushed. This confirmed the integrity of the reactor feed.

In between individual reactor runs additional blanks acquisitions were conducted in an analogous manner, particularly when multiple different reactor positions were investigated sequentially. These blanks aimed to verify and prevent potential cross-contamination by visualising the duration of product traces in the fluidic setup until the analytical loop, subsequent to the reactor line. Then, the switch to the next reactor position was only done, as soon as the reactor line was washed and only reactant and buffer signal remained (B; n=1-5, depending on signal intensities).

Reactor run: Past the previously described reactor pump and sample feed blanks, the selector valves were switched to the next reactor position, which was connected to a packed µreactor (for general

µreactor description see section S1.1). At this position, long-term experiments could be conducted to monitor the stability of the catalytic material and evaluate the overall performance (see Fig. S12 C). The duration of these experiments was determined by the lifetime of the catalytic material, as well as the size of the reactant sample loop and the flow rate of the reactor pump. By that, multiple µreactors could be compared by sequentially addressing different reactor positions.

Validation: It was generally observed that when the selector valves were switched to a different reactor position, there was a time delay of approx. one acquisition (approx. 10 min) until the analytical feedback adjusted to the new reactor position. This delay was considered during subsequent data evaluation, considering it as a measurement from the previous conditions. This effect accounted for the applied flow rates of 0.2 µl/min for the reactor flow and 2 µl/min for the dilution past the reactor.

Reactor washing: At the end of all reactor runs, washing cycles were conducted by turning off the sample feed and flushing the respective reactor positions. Here, LC-MS-measurements were also conducted, which enabled to observe the process. Similarly, when using the autosampler to evaluate different sample input for different reactor positions, the overall line was flushed before injecting the next sample and switching to the next reactor (by switching to a blank capillary position and observed the flushing process).

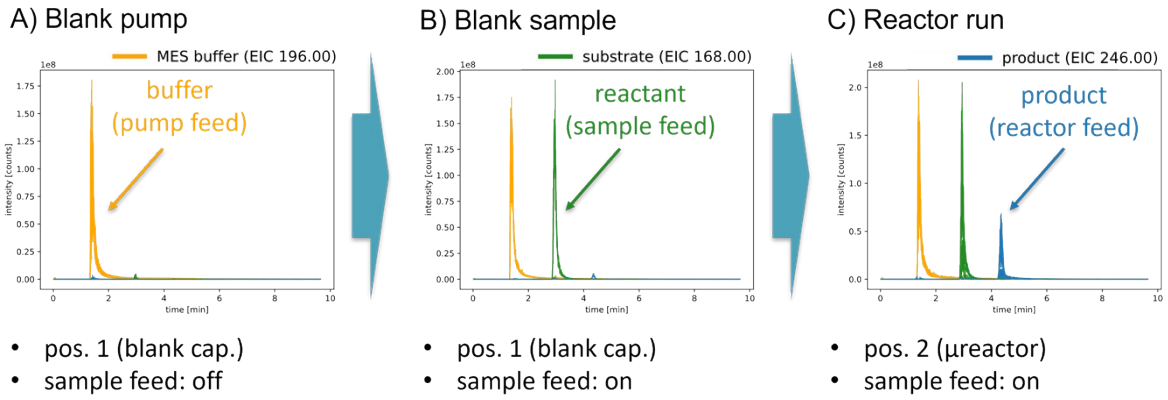

Fig. S12 Visualization of the different LC/MS chromatograms as signal feedback at different run stages. **A)** First, blank measurements of pump feedback are shown, containing only the buffer peak. **B)** Then, blank measurements after adding the reaction sample are depicted. **C)** Finally, after switching to the flow path to the packed-bed µreactor also the product peak can be detected.

3.2. Data evaluation workflow

For data evaluation, all monitored EIC-traces from the individual MS-files as recorded by the Bruker AmaZon SL mass spectrometer were exported in “Bruker Data Analysis” into .xy or .csv-file format using a custom postscript method. Similarly, the pressure data, as recorded from the analogous detection channels from the “Colibrick”-box, were exported by the “Clarity”-software into a .csv file format. These acquired files were then then imported and processed in Python as “Panda DataFrames” using “Jupyter Notebooks”. The data was then sorted according to the individual EIC-traces (buffer, reactant, product, etc.) and organized based on the corresponding sequences structure of the run (blanks, reactor runs, etc.). The individual separated peaks were then integrated by time range definition and various parameters such as intensity, peak areas, and retention times evaluated. The calculated areas provided then insight into further reaction parameters such as the product signal fraction or overall byproduct formation. By comparing the reactant intensities of the sample blanks before and during the reactor runs it was possible to get an insight into reactant conversion. The entire run, including the individual subparts, was then examined regarding signal stability, and blank acquisitions were checked for contaminations. Finally, the sorted data and resulting “DataFrames” were exported as .xlsx files and visualized using matplotlib as .svg and .png image files. The respective workflow is illustrated in Fig. S13.

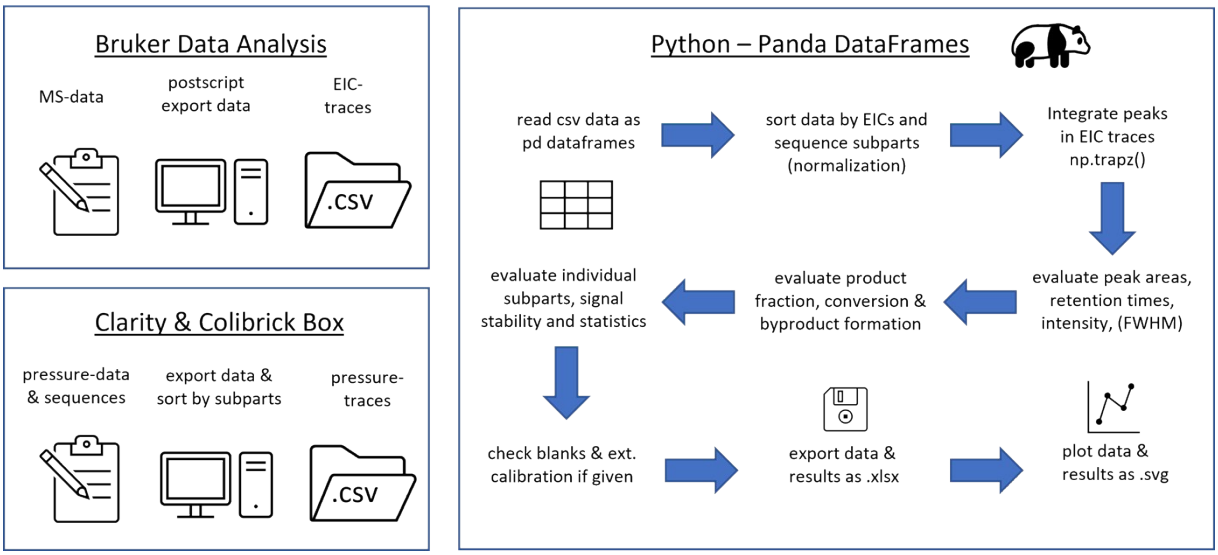

Fig. S13 Workflow for processing the acquisition data as described above. This includes the export of the MS- and pressure data into .csv formats and subsequent evaluation in a Python-based workflow using "Panda DataFrames" and "Matplotlib" for plotting.

4. Enzyme preparation, immobilisation process and model reaction

4.1. General information

NH_2-coated ProntoSil particles (size 5 µm) were bought from Bischoff (DE). Protein concentrations were determined using a Nanodrop 2000c spectrophotometer (Thermo Scientific, ε (*Ci*VHPOHalo) = 150480 M^{-1} cm^{-1}). UV/Vis spectra were recorded on a BioTek® Eon spectrophotometer using 96-well polystyrene microplates (Brand® F-bottom, UV-transparent, pureGrade™). For protein purification, an ÄKTA FPLC system (GE Heatlhcare) with Histrap FF crude column (Cytiva) or HiPrep™ 26/60 Sephacryl S-200 HR column (Cytiva) was used. The solvent used were p.a. grade. Gas chromatography (GC) was performed on a Varian 3900 gas chromatograph with a Varian Saturn 2000 mass spectrometer. A HP5 low Bleed GC column with a constant flow rate of 1 mL min^{-1} with Hydrogen as carrier gas was used. A temperature gradient starting from 60 °C to 250 °C over 20 min was applied.
The following chemicals were purchased: Ammonium bromide (Sigma, 99.0%), 2-chloro-5,5-dimethyl-1,3-cyclohexandione (fisher scientific, 98%), ethyl 3,5-dimethyl pyrrole-2-carboxylate (BLD Pharm, 99.94%), 2-(*N*-morpholino)ethanesulfonic acid (TCI chemicals, >99.0%), sodium orthovanadate (Acros, ≥99%), tris(hydroxymethyl)aminomethane (Sigma, ≥99.9%).

4.2. Enzyme production, particle preparation and enzyme immobilisation

- *Heterologous production of CiVHPOHalo:*

The vanadium dependent haloperoxidase (*Ci*VHPO) gene (Genbank accession number CAA59686) was introduced into the pET22 Plasmid, containing an *N*-terminal HaloTag®, by Sequence and Ligation Independent Cloning (SLIC). The successful SLIC reaction was verified by Sanger sequencing (Genewiz, Leipzig, DE). The following primer were used (SLIC homology region is underlined):

*Ci*VHPO_Halo_for	5' GAAAGCGGCCGCGGGCAGCGTAACGCCAATTCCG 3'
*Ci*VHPO_Halo_rev	5' CTTTGTTAGCAGCCGGATCCTATGGCGCTTCTTTGACAACCG 3'
*Ci*VHPO_Halo_Plasmid_for	5' GTCAAAGAAGCGCCATAGGATCCGGCTGCTAAC 3'
*Ci*VHPO_Halo_Plasmid_rev	5' GAATTGGCGTTACGCTGCCCGCGGCCGCTTTC 3'

The *Ci*VHPOpET22 plasmid was introduced into competent BL21 (DE3) *E.* coli cells (Thermo Fisher Scientific, Massachusetts, US) through transformation. All media used for expression contained a final

concentration of 100 µg/mL^{-1} ampicillin. Typically, 0.5-1.0 L of TB-media with 10% glycerol (v/v) were inoculated with a 1-2 mL overnight culture of LB-media. The cells were grown at 37 °C and 200 rpm shaking until an optical density OD_{600} of 0.6 was reached. Protein production was induced by addition of IPTG to a final concentration of 0.2 mM, and the cells were then incubated at 18 °C and 200 rpm shaking for 18 h. The cell pellet was collected by centrifugation (5000 g, 5 min, 4 °C) and washed with a 0.9% NaCl solution. Cell lysis was achieved by sonification (3 s turned on, 9 s off, total sonication time of 5 min at 55% intensity; Sfx150, Branson Ultrasonics, Connecticut, US) on ice. For that purpose, the pellet was resuspended in 10 mL g^{-1} pellet lysis buffer (10 mM imidazole, 300 mM NaCl, 50 mM TrisHCl pH 8.0, 10% glycerol) and 1 mM PMSF as well as 100 µg/mL lysozyme were added before sonification. After centrifugation (8100 g, 60 min, 4 °C), the supernatant was purified on a ÄKTA start (Cytiva, Massachusetts, US) with 1 mL HisTrap FF Crude column (Cytiva). The elution fractions (see Fig. S14) containing the enzyme were subjected to a buffer exchange column PD-10 (GE healthcare). The storage buffer used contained 50 mM Tris pH 7.0 and 100 µM Na_3VO_4. A gel filtration step was employed as second purification step on a ÄKTA start with a HiPrep™ 26/60 Sephacryl S-200 HR column (Cytiva). For that purpose, storage buffer was used with a flow rate of 1.5 mL/min (see Fig. S15). The enzyme concentration was determined using a NanoDrop™ 2000 (Thermo Fisher Scientific). Typically, 6-9 mg SEC purified *Ci*VHPOHalo was obtained per 1 L culture. The enzyme was frozen in liquid nitrogen and stored at -80 °C.

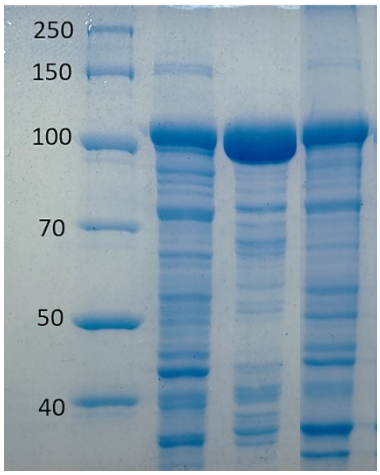

Fig. S14 SDS PAGE of *Ci*VHPOHalo after IMAC purification. Rows from left to right: Marker (sizes shown in kDa), lysate before IMAC purification, combined elution fractions after elution from IMAC purification, pellet fraction after lysing and centrifugation.

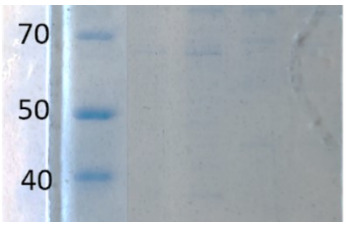

Fig. S15 SDS PAGE of *Ci*VHPOHalo after SEC purification. Rows from left to right: Marker (sizes shown in kDa), row 2-5 are all *Ci*VHPOHalo containing fractions in a high purity.

- *Chloroalkane linker synthesis:*

The HaloTag™-targeting chloroalkane linker was synthesized as reported by Meade *et al*.[13] (The structure **S1** is shown below)

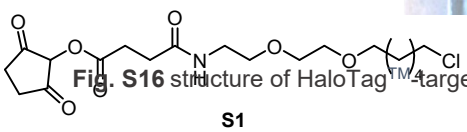

S1

Fig. S16 structure of HaloTag™-targeting chloroalkane linker **S1** used in the immobilisation process.

- *CiVHPOHalo immobilisation protocol:*

The NH_2-coated ProntoSil particle, typically 10 mg, was suspended in EtOH (100 µL mg^{-1} of carrier), the linker **S1** (as shown above), freshly prepared 100 mM solution in EtOH, 10.4 µL mg^{-1} of carrier) and NEt_3 (0.5 µL mg^{-1} of carrier) were added, and the mixture was incubated at 30 °C and 1200 rpm shaking for 16 h. After centrifugation (7000 g, 2 min), the supernatant was removed, and the particles were

washed with EtOH (2x 100 µL mg^{-1} of carrier). Next, *Ci*VHPOHalo (1.59 µL mg^{-1} of carrier, 3.142 µg/µL stock concentration) and buffer (48.41 µL mg^{-1} of carrier, containing 50 mM Tris pH 6.0, 100 µM Na_3VO_4) were added. The reaction mixture was incubated for 1 h at 25 °C and 1200 rpm shaking, followed by removing the supernatant through centrifugation (7000 g, 2 min). Two washing steps were performed using the buffer (50 µL mg^{-1} of carrier, 50 mM Tris pH 6.0, 100 µM Na_3VO_4).

- *Quantification of linker loading on NH_2-particles by Kaiser Test*

To determine how much chloroalkane linker was added to the NH_2-coated Si particles in the immobilisation process, the Kaiser Test was used to quantify free amine groups before and after the addition of the linker.[14] For calibration, defined amounts of NH_2-coated ProntoSil particles (ranging from 0.50-4.00 mg) were applied in the Kaiser Test, and the measured absorbance at 530 nm was plotted against the quantity of particles applied (Fig. S17). A linear correlation between absorbance and used particle amount was observed in this range. After coating the particles with the HaloTag™-targeting chloroalkane linker **S1**, the Kaiser test then quantified the unreacted amine groups, and the percentage of linker loading was calculated.

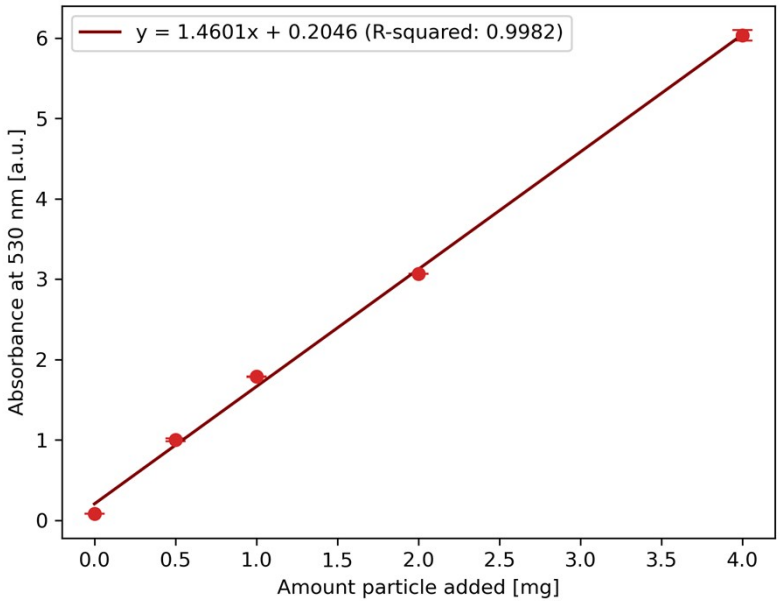

Fig. S17 Calibration slope of ProntoSil particles (amount added between 0.50 and 4.00 mg) with the Kaiser Test. Absorbance at 530 nm was measured and plotted against the amount of ProntoSil used. The linear equation rearranged to x = 0.6849y – 0.1401 was used to determine unreacted amine functionalities after reaction with the HaloTag™ linker. Linker loading was then calculated with the following equation:

$$linker\ loading\ (in\ \%) = \frac{amine\ on\ particle\ after\ immobilisation}{amine\ on\ particle\ before\ immobilisation} * 100$$

An additional calibration with varying amounts of n-octylamine (ranging from 0.25-3.0 µmol) was conducted to determine absolute amine group amounts by the Kaiser Test. Then, the measured absorbance at 570 nm was plotted against the applied concentration of *n*-octylamine to obtain a calibration slope (see Fig. S18). This slope was used to quantify amine functionalities on ProntoSil particles before and after linker coating and to determine the absolute amount of chloroalkanes coated to the particles. After the immobilisation process, 1 mg of ProntoSil particles were usually coated with 473 nmol – 494 nmol of HaloTag™-targeting chloroalkane linker **S1**.

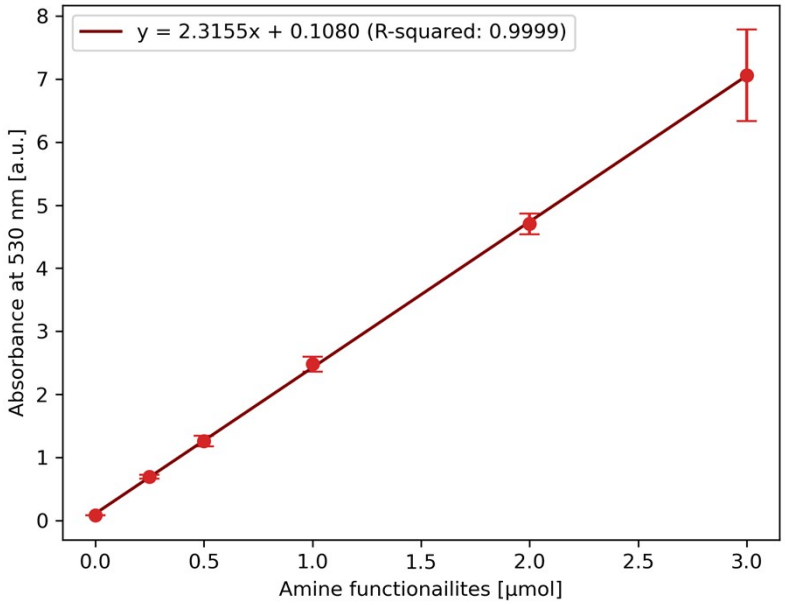

Fig. S18 Calibration slope of *n*-octylamine (ranging from 0.25-3.0 µmol) with the Kaiser Test. Absorbance at 530 nm was measured and plotted against used *n*-octylamine. The linear equation rearranged to x = 0.4319y – 0.0466 was used to quantify amine functionalities [µmol] of particles corresponding to the measured absorbance in the Kaiser Test.

- *Determination of CiVHPOHalo supernatant concentrations by Monochlorodimedone (MCD) assay:*

The spectrophotometric monochlorodimedone (MCD) assay,[15] commonly used to measure haloperoxidase activity, was used here for the determination of *Ci*VHPOHalo concentrations of the supernatants after the immobilisation and washing protocol. A typical MCD assay (0.30 mL) contains MES buffer (50 mM, pH 6.0), MCD (50 µM, dissolved in 2 M NaOAc solution), KBr (200 mM), Na_3VO_4 (300 µM), and H_2O (176 µL). The assay was initiated by adding *Ci*VHPOHalo (1 µL, either directly from the supernatant or diluted samples) and H_2O_2 (10 mM). The decrease in absorbance at 290 nm was monitored for 10 min at 30 °C while shaking at 400 rpm.

First, for *Ci*VHPOHalo quantification of the supernatants, a calibration slope with defined final enzyme concentrations ranging from 44.1 fmol to 1.38 fmol *Ci*VHPOHalo was measured in triplicates using the MCD assay. Plotting the decrease of absorbance at 290 nm over one minute (y-axis, see Fig. S19) against the amount of enzyme applied (x-axis) shows a linear correlation. To determine CiVHPOHalo concentrations in the supernatants after immobilization, a typical MCD assay with 1 µL of the supernatant added was conducted. Based on the absorbance decrease over one minute, the concentration in the supernatant was calculated using the linear equation of the calibration plot (see Fig. S19)

Finally, enzyme loading on the particles was calculated using the following equation:

$$Enzyme\ loading\ (\mu g\ enzyme\ mg^{-1}\ of\ particles) = amount\ enzyme\ added\ before\ - amount\ enzyme\ in\ washing\ steps$$

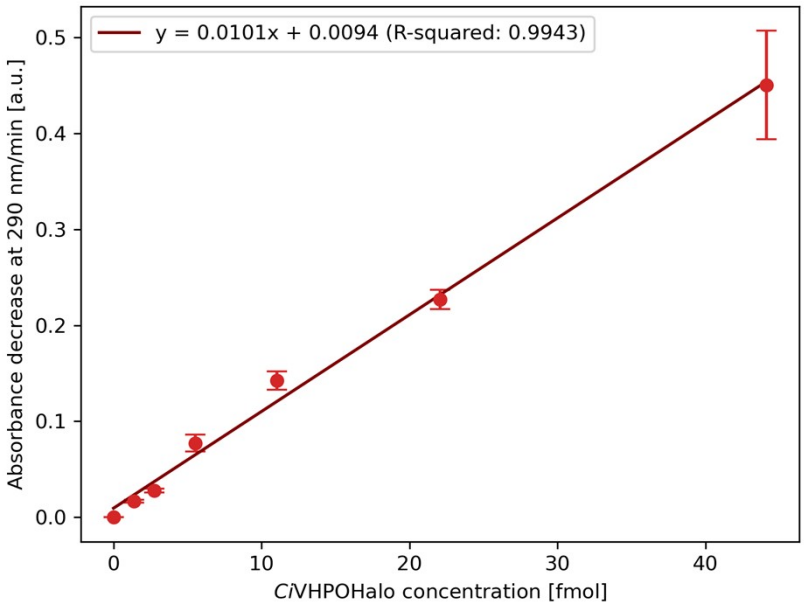

Fig. S19 Calibration slope of *Ci*VHPOHalo (conc. added between 44.1 fmol to 1.38 fmol *Ci*VHPOHalo) measured using the MCD Assay. The decrease of absorbance at 290 nm was measured over 10 min, and the decrease of absorbance min^{-1} was plotted against the used *Ci*VHPOHalo concentration. The linear equation of rearranged to x = 1.922y + 0.0037 was used to calculate unknown *Ci*VHPOHalo concentrations.

- *Comparing enzyme activity of immobilised and in solution CiVHPOHalo*

To compare the enzyme activity of *Ci*VHPOHalo immobilised on ProntoSil compared to in solution *Ci*VHPOHalo, the enzymatic brominating reaction of ethyl-3,5-dimethyl pyrrolecarboylat (**1**) was followed over time. For that, ethyl-3,5-dimethylpyrrolecarboylat (**1**, 3.20 µmol, 1.0 eq.), NH_4Br (16.0 µmol, 5.0 eq.), Na_3VO_4 (320 nmol, 0.10 eq.), MES Buffer (50 mM pH 6.0, 8 µL), ACN (11.1 µL), H_2O (59.8 µL for homogeneous reaction, 48.6 µL for heterogeneous reaction) and H_2O_2 (3.20 µmol, 1.0 eq.) were mixed. The reactions were started by adding immobilised *Ci*VHPOHalo (12.5 µL, suspension in H_2O, loading of 4.08 µg *Ci*VHPOHalo mg^{-1} particle) or in solution *Ci*VHPOHalo (1.30 µL, 3.142 mg mL^{-1} stock solution). Reactions were stopped after 5, 10, 15, 20, 25, or 30 min by adding the mixture of sat. NaCl (90 µL), sat. NH_4Cl (90 µL) and EtOAc (250 µL). All reactions were conducted as triplicates. After separating the phases, 50 µL of the organic phase was diluted with 110 µL EtOAc, and the sample was measured using GC-MS. The ratio of peak areas for starting material **1** and brominated product **2** was plotted against the reaction time (see Fig. S20). With the slopes obtained, a remaining activity of 68% for *Ci*VHPOHalo immobilised on ProntoSil particles compared to soluble *Ci*VHPOHalo was calculated.

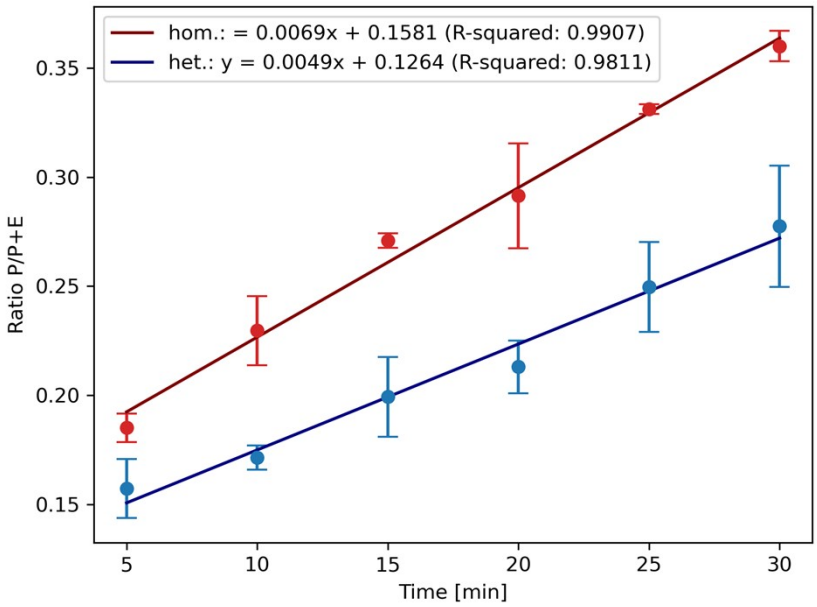

Fig. S20 Ratio of integrals for product **2** to product **2** + starting material **1** measured by GC-MS and plotted against the reaction time. Blue: *Ci*VHPOHalo immobilized on ProntoSil chloroalkane particles, Red: *Ci*VHPOHalo in solution. The reaction of ethyl 3,5-dimethyl pyrrole-2-carboxylate (**1**) to ethyl-4-bromo-3,5-dimethyl pyrrole-2-carboxylate (**2**) was examined.

4.3. Model reaction, byproduct formation, and peak identification

- *Model biotransformation:*

As a model reaction for the developed integrated system, the bromination of ethyl 3,5-dimethyl pyrrole-2-carboxylate (**1**) to ethyl-4-bromo-3,5-dimethy lpyrrole-2-carboxylate (**2**) was investigated. The reaction equation is shown in Scheme S1. In general, the substrate was mixed with different concentrations of NH_4Br, Na_3VO_4, MES buffer (pH 6.0), and H_2O_2 in an overall solvent mixture of ACN/H_2O 40/60 (v/v) (more information see Table S1). Immobilized *Ci*VHPOHalo was applied as a biocatalyst for flow reactions, while soluble *Ci*VHPOHalo was used as an enzyme catalyst in batch reaction.

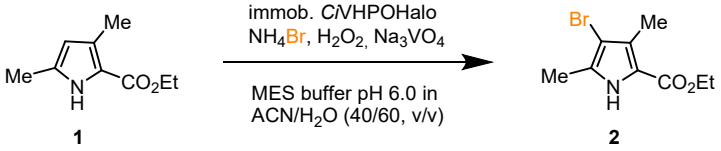

Scheme S1 Reaction equation of the vanadium-dependent haloperoxidase *Ci*VHPOHalo catalysed bromination of ethyl-3,5-dimethylpyrrole-2-carboxylate (**1**) to ethyl-4-bromo-3,5-dimethylpyrrole-2-caboxylate (**2**) as model biotransformation for the integrated system. The reaction was carried out inspired by the literature.[16]

All the different compositions of the reaction mixture tested during this study are listed in detail in Table S1.

Table S1 Table of the different reaction mixtures tested. The reaction mainly was tested with the initial composition (rct. mix 1). The other mixtures (rct. mix. 2-4) were tested in the multi-reactor section for testing different mixtures on multiple connected µreactors. Decreasing the substrate concentration but increasing hydrogen peroxide equivalents (rct. mix 5) is leading to a higher conversion rate, but also to byproduct **S2**-**S5** formation as discussed in the next section. Significant increase of the hydrogen peroxide fraction instead leads to product **2** formation without enzyme addition (composition not shown, using up to 230 mM H_2O_2, otherwise maintaining the composition as rct. mix. 1).

Components	Mix 1 (org.)	Mix 2 (Br--, H_2O_2++)	Mix 3 (Br--, H_2O_2++, Na3VO4++)	Mix 4 (Br--, H_2O_2++, MeCN++)	Mix 5 (sub--)
Ethyl *3,5*-dimethyl pyrrole-*2*-carboxylate (**1**, substrate)	10 mM	10 mM	10 mM	10 mM	3.3 mM
NH_4Br (bromide source)	70 mM	17.5 mM	17.5 mM	17.5 mM	70 mM
Na_3VO_4 (enzyme cofactor)	1 mM	1 mM	2 mM	1 mM	1 mM
2-(N-morpholino) ethane sulfonic acid (MES-buffer, pH 6.0)	50 mM	50 mM	50 mM	50 mM	50 mM
H_2O_2 (oxidant)	10 mM	20 mM	20 mM	20 mM	10 mM
MeCN composition	40 %	40 %	40 %	70 %	40 %

- *Byproduct formation:*

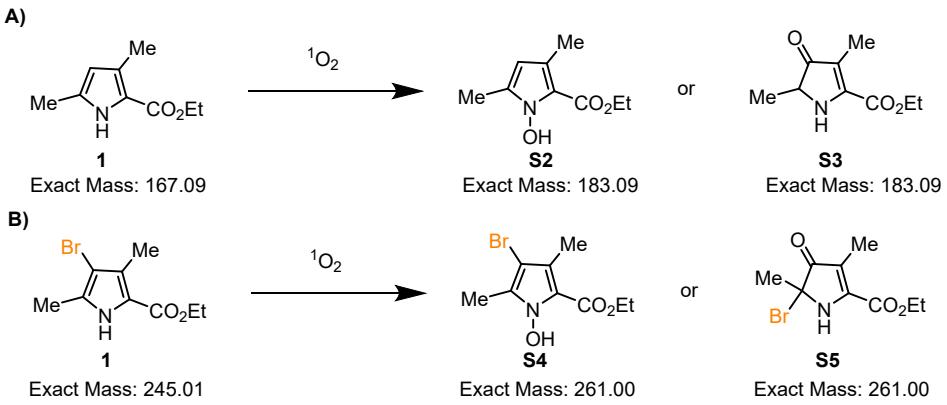

Scheme S2 Suggested byproduct structures **S2**-**S5** that could explain the additional observed peaks at increased hydrogen peroxide concentration in relation to the reactant **1**. The two potential byproducts are formed by reacting with singlet oxygen. **A)** Suggested side reaction for the reactant **1** ($[M+H]_{reactant}$+16); **B)** Suggested byproduct **S4**+**S5** of the brominated product **2** ($[M+H]_{product}$+16).

For reaction conditions with excess hydrogen peroxide concentration (3 eq. instead of 1 eq.), two additional byproducts **S2**-**S5** were observed ($[M+H]_{reactant}$+16 and $[M+H]_{product}$+16). Those compounds **S2**-**S5** can be suggested as oxygenated byproducts of the reactant **1** and product **2**. During the reaction mechanism, HOX is formed by the enzyme as a reactive species. According to the literature, the remaining unreacted species HOX can react with a second hydrogen peroxide equivalent to form singlet oxygen ($^1O_2$). This mechanism was also reported for the *Ci*VHPO.[17] This highly reactive singlet oxygen can then be added to the substrate, forming the corresponding peroxides that then collabs to the oxygenated products **S2**-**S5** shown above.[18] No byproduct formation was observed by reducing the hydrogen peroxide concentration relative to reactant (1:1 ratio).

- *Peak identification:*

When monitoring the model reaction, three dominant peaks were observed in the LC/MS chromatogram, as shown in Fig. S21 A. Those peaks could be referred to as the buffer, reactant **1**, and product **2**. The buffer peak was utilized as a dead time marker (tr = 1.4 min) and appeared as monomeric as well as dimeric (dominant) species of the MES-buffer ($[M+H]^+$ = 196, $[2M+H]^+$ = 391) in the mass spectra. The next eluting peak was the reactant species **1** (tr = 3.0 min, $[M+H]^+$ = 168). The brominated product **2**

eluted last and was easily recognized in the spectra by the isotope pattern unique for bromine atoms (tr = 4.4 min, $[M+H]^+$ = 246, spectra shown in Fig. S21 A).

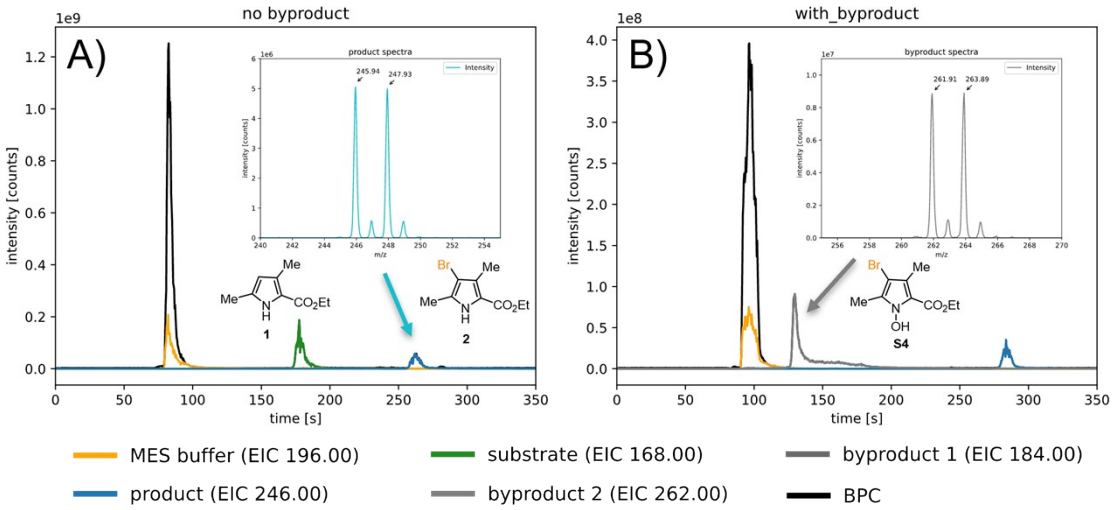

Fig. S21 Acquired LC/MS chromatograms are shown here for peak identification. For the different reaction components and the product, the extracted ion chromatograms (EICs) are shown (here, the EIC of only one bromine isotope is shown in the chromatogram). Furthermore, the base peak chromatogram (BPC) is shown as an overlay. **A)** Peaks were observed for the reaction mixture with 10 mM reactant **1** (rct. mix. 1, see Table S1). Furthermore, the respective spectra of the brominated product **2** are shown (showing the characteristic isotopic bromine pattern; $[M+H]^+$ = 246). For the first peak, corresponding to the MES buffer, the dimeric species is more abundant than the monomeric one as shown in the BPC ($[M+H]^+$ = 196, $[2M+H]^+$ = 391). **B)** Peaks for the reaction mixture with 3.3 mM reactant **1** but 10 mM H_2O_2 (rct. mix. 5, see Table S1) were observed. Here, due to an excess of hydrogen peroxide complete, complete conversion could be observed, but additional byproduct formation is also observed ($[M+H]^+$ = 262), as explained in the previous section. Reactor: packed with *Ci*VHPOHalo on ProntoSil particles (Ø 5 µm, loading f_A = 20.6 µg·mg^{-1}, f_B = 10.4 µg·mg^{-1}), rct. pump: 0.2 µl·min^{-1} 50 mM MES-buffer (residence time approx. 40 s, flushing sample loop with 2 µl·min^{-1} for 3 min at start; dilution: 2 µl·min^{-1} MeCN:H_2O, 60:40 vol% with 50 mM MES as sample); Analysis: Zorbax Eclipse Plus (C18, 4.6x100 mm, 3.5 µm, Agilent), 600 µl·min^{-1} MeCN:H_2O (70:30 vol% with 0.1% FA, 60 bar at pump, 2 µl injection volume

5. Additional information on performed experiments and applications

5.1. Part_1 - Setup and immobilized enzyme evaluation

- *Single reactor runs – enzyme immobilisation:*

To evaluate the activity and immobilisation efficiency of the immobilised enzyme multiple different long-term runs were conducted. For that purpose, either the immobilised enzyme or blank species including either solid support with enzyme, but without prior linker addition, or particles without enzyme addition, were packed into a µreactor channel and monitored during a constant reactant sample feed (either 10 mM or 3.3 mM reactant **1**) for approx. 22 h while sampling the reactor effluent to online LC/MS analysis each 15 min (approx. 85-100 chromatograms for each run shown). The different runs are shown in Fig. S22 and briefly discussed in the following. For each run a waterfall plot of all chromatograms, the integrated areas, as well as the fraction of the integrated product peak area in relation to the reactant peak area is shown (product area fraction = PF = P_area/(P_area+E_area), only one brominated product isotope area considered here for visualization and comparison).

First, a run is shown **(A)**, where a chip was packed with ProntoSil particles for which the linker was attached, but without enzyme addition reactant **1** (rct. mix. 1, see Table S1). As expected, no significant product **2** formation could be observed for this blank acquisition (PF > 0.01). Secondly **(B)**, a second run was conducted using particles with added enzyme, but without prior linker coupling. Thus, only non-

specific binding of the enzyme to the particle can be present. For this run a product **2** formation could be observed (initially PF = 0.4; rct. mix. 1), slowly decreasing over the first 5 h (reaching a stable PF of 0.23). Afterward **(C)**, the fully prepared, with Halo-tag immobilised enzyme was tested in a packed-bed reactor using 10 mM reactant **1** (rct. mix. 1), showing a significantly higher conversion rate which slowly decreased over the observed time (mean PF = 0.55). Finally **(D)**, another run with fully immobilised enzyme is presented but less reactant **1** concentration was tested (3.3 mM reactant **1**, 10 mM H_2O_2, rct. mix. 5). For this run, full product conversion could be observed (PF = 1). However significant byproduct formation could be observed as discussed in section S4.3. Due to the high activity, another blank run with particles without enzyme addition was similarly conducted (not shown; rct. mix. 5; mean product area fraction of 0.02). This blank run was performed to assign the product formation solely to the enzyme activity, as significant product formation without enzyme addition was observed in pre-experiments at significantly higher hydrogen peroxide concentrations (not shown; 10 mM reactant **1**, 230 mM H_2O_2).

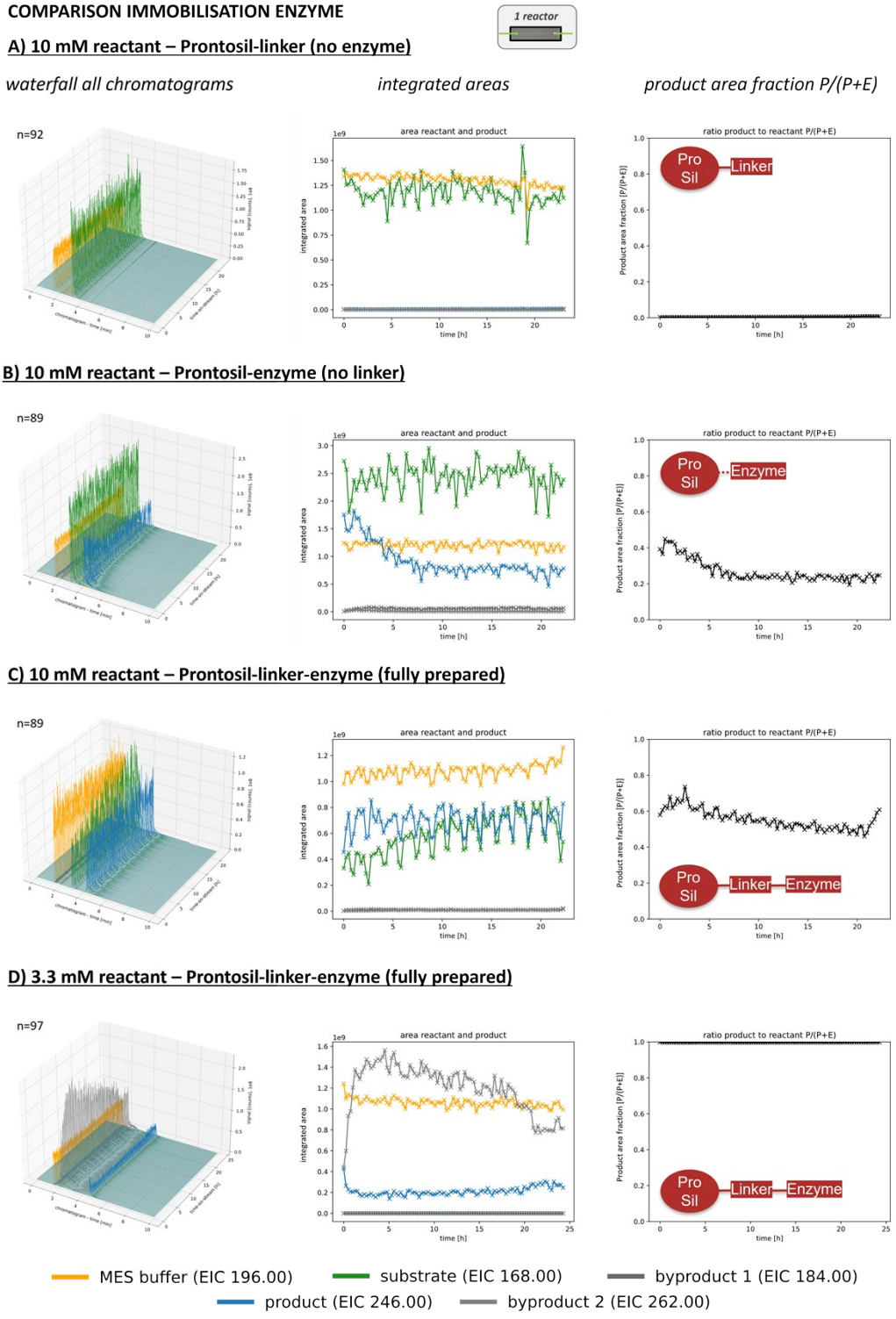

Fig. S22 Different long-term single packed-bed µreactor runs including blank runs without linker or enzyme addition as well as runs at two different reactant **1** concentrations (each run approx. n=85-100, 23-24 h, sampling each 15 min; only one brominated product isotope considered for visualization) **A)** run using particles with coupled linker, but without enzyme addition. (rct. mix. 1, 10 mM, see Table S1); **B)** run using particles with enzyme addition, but without prior linker coupling showing only unspecific enzyme binding (rct. mix. 1, 10 mM); **C)** run using fully prepared particles. (rct. mix. 1, 10 mM); **D)** run using fully prepared particles but lower substrate concentration, showing full conversion, but significant byproduct formation as discussed in Section S4.3 (rct. mix. 5, 3.3 mM). Similarly, as for 10 mM, almost no product formation was visible for blanks without immobilized enzyme. Reactor: packed with *Ci*VHPOHalo on ProntoSil particles (Ø 5 µm, loading $f_{C,D}$ = 10.4 µg·mg^{-1}, f_B = 16.1 µg·mg^{-1}), rct. pump: 0.2 µl·min^{-1} 50 mM MES-buffer (residence time approx. 40 s, flushing sample loop with 2 µl·min^{-1} for 3 min at start; dilution: 2 µl·min^{-1} MeCN:H_2O, 60:40 vol% with 50 mM MES as sample); Analysis: Zorbax Eclipse Plus (C18, 4.6x100 mm, 3.5 µm, Agilent), 600 µl·min^{-1} MeCN:H_2O (70:30 vol% with 0.1% FA, 60 bar at pump, 2 µl injection volume.

- *Consecutive reactor runs – reproducibility:*

Then, multiple consecutive reactor runs were carried out with fully prepared particles (10 mM and 3.3 mM reactant **1**). For this purpose, the reactor was flushed over-night after each run. Then, before introducing a fresh reactant sample, the reactor effluent was measured in blank acquisitions to verify that no residual product **2** or reactant **1** traces were present. The two runs are shown in Fig. S23 and briefly discussed in the following.

For the first runs (**A**, rct. mix. 1, 10 mM, see Table S1), a relatively stable but slowly decreasing product formation was visible for the three conducted runs (mean PF of 0.55, 0.44 and 0.37; here only one brominated product isotope considered for comparison). For the other runs (**B**, rct. mix. 5, 3.3 mM), full conversion could be observed for the first run under significant byproduct formation (as shown in Fig. S22 D and discussed in section S4.3; PF = 1). However, drastic decrease of the enzyme activity was observed in the second run (down to PF = 0.08 after 25 h) and almost no remaining conversion in the third run (mean PF of 0.03). This could result from potential oxidative deactivation of the enzyme, due to the increased formation of singlet oxygen (as discussed in section S4.3). For better comparability of different reaction parameters all subsequent runs were performed using rct. mixes with 10 mM reactant **1**.

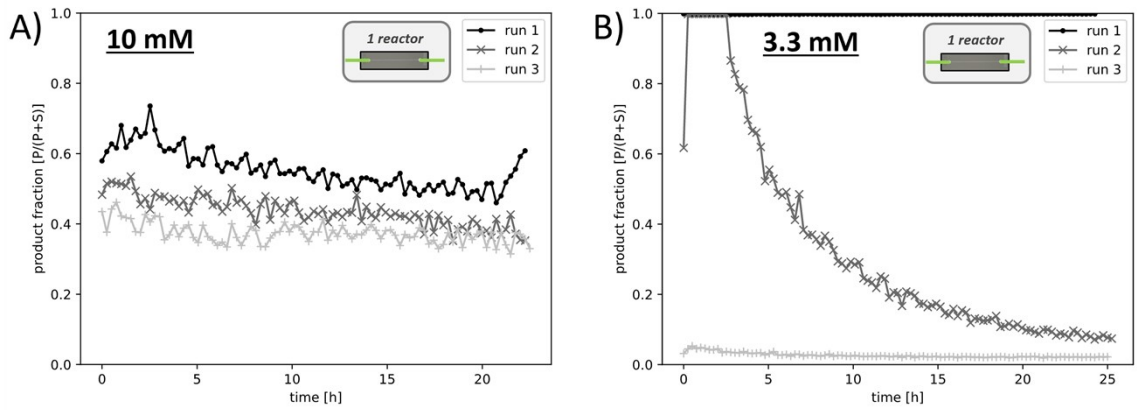

Fig. S23 Comparison of three consecutive runs of a freshly packed chip with either 10 mM or 3.3 mM reactant **1**. The chip was flushed over-night between each run and blank measurements were acquired to assure no cross-contamination between the individual runs (each run approx. n=85-100, 23-24 h, sampling each 15 min; only one brominated product **2** isotope area considered here for visualization). **A)** Using a mixture with 10 mM reactant **1** (rct. mix. 1, see Table S1) resulted in a relatively stable product **2** conversion, which was decreasing in between the individual runs **B)** Using a mixture with 3.3 µM reactant **1** instead (rct. mix. 5, see Table S1) resulted in full conversion for the first run, with significant decrease in the following runs. As shown in Fig. S22 D during the initial run extensive byproduct **S2**-**S5** formation could be observed. Reactor: packed with *Ci*VHPOHalo on ProntoSil particles (ø 5 µm, loading f_{AB} = 10.4 µg·mg^{-1}), rct. pump: 0.2 µl·min^{-1} 50 mM MES-buffer (residence time approx. 40 s, flushing sample loop with 2 µl·min^{-1} for 3 min at start; dilution: 2 µl·min^{-1} MeCN:H_2O, 60:40 vol% with 50 mM MES as sample); Analysis: Zorbax Eclipse Plus (C18, 4.6x100 mm, 3.5 µm, Agilent), 600 µl·min^{-1} MeCN:H_2O (70:30 vol% with 0.1% FA, 60 bar at pump, 2 µl injection volume.

5.2. Part_2 - Multi-reactor valves integration

- *Complex single reactor run with blank acquisitions:*

During this run a single reactor was monitored with constant sample feed in a long-term-experiment. In contrast to the previously shown runs two additional selector valves were integrated to enable automated switching between different reactor positions in single runs. For the following run a single packed-bed µreactor (ProntoSil with *Ci*VHPOHalo) and a blank capillary were connected and subsequently investigated in multiple sequential function blocks. During each function multiple LC-MS

measurements were acquired to monitor the reactor effluent. The respective sequence used is depicted in Fig. S24 and shortly discussed below. Afterward all resulting chromatograms are depicted together in a waterfall chromatogram in Fig. S25. Then, the respective subparts are discussed individually, regarding the integrated areas and product area fraction for reactor evaluation.

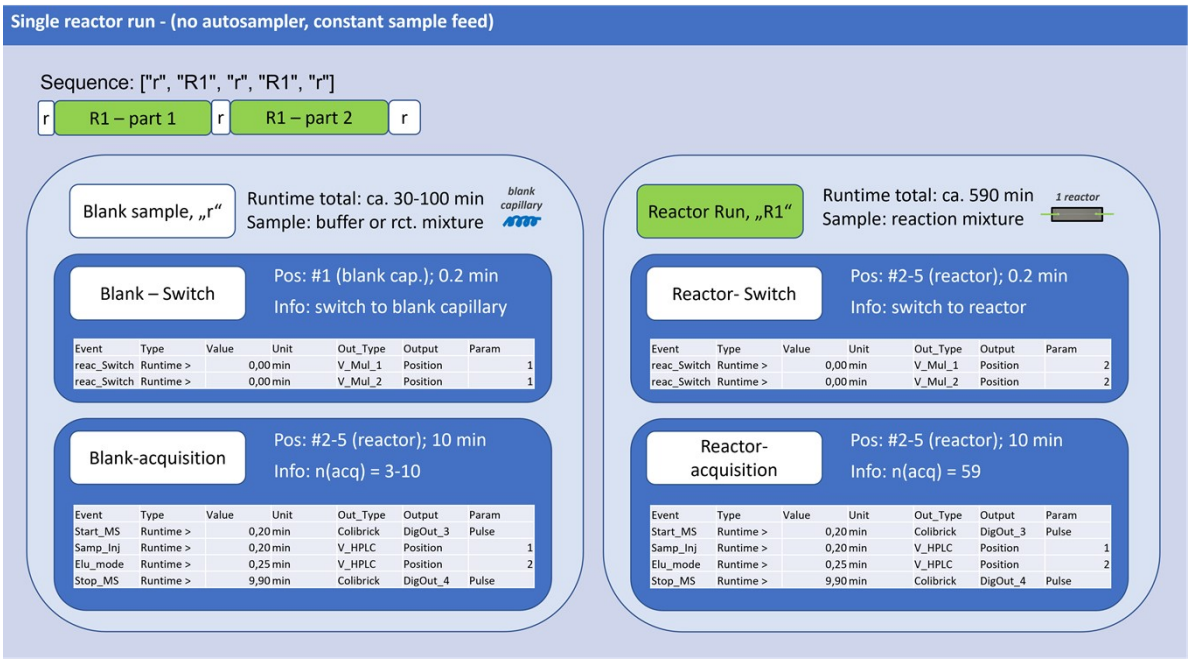

Fig. S24 Sequence performed for testing a packed-bed µreactor with constant sample feed for approx. 22 h in total. Before, at the middle and at the end of the run multiple blank acquisitions were acquired by switching from the µreactor to a blank capillary to observe either the pump or the sample feed. shown are the utilized event tables as defined in the ”Clarity” software for each method/function block as described in Fig. S11. “r”: blank sample, “R1”: reactor run.

At the beginning of the run, the sample feed was coupled in by switching the sample valve located before the reactor selection valves. The sample loop connected to the valve was filled externally through a syringe adapter before the run. Then, the sequence was started, and the reactor position was set to a blank PEEK capillary, to acquire sample feed blank measurements (**„Blank sample, „r”***;* Fig. S26 A). Here, the overall signal stability and background was observed and observed for potential contaminations. During later runs additional blank acquisitions were also acquired before coupling in the sample feed to just observe the general pump feed (as shown before in Fig. S12 A). Then, the reactor position was switched to the µreactor to be tested and monitored for approx. 10 h of operation (**„Reactor 1”**, **„R1”***;* Fig. S26 B). Then, the reactor position is switched back to the blank capillary monitoring only the sample feedback (**„Blank sample”**, **„r”***;* Fig. S26 C), observing the signal stabilities and testing for carry-over effects in the sample loop of the valve connected to the analytical system. As expected, the respective blank chromatograms showed no observable product **2** signal traces. Afterward, the reactor position was switched back to the previously running packed-bed µreactor for further investigation and approx. 10 h of operation (**„Reactor 1”**, **„R1”***;* Fig. S26 D). At the end of the run further blank measurements were conducted by switching back to the blank capillary (**„Blank sample”**, **„r”***;* Fig. S26 E). For this run, none of the discussed byproduct **S2**-**S5** signals were observable.

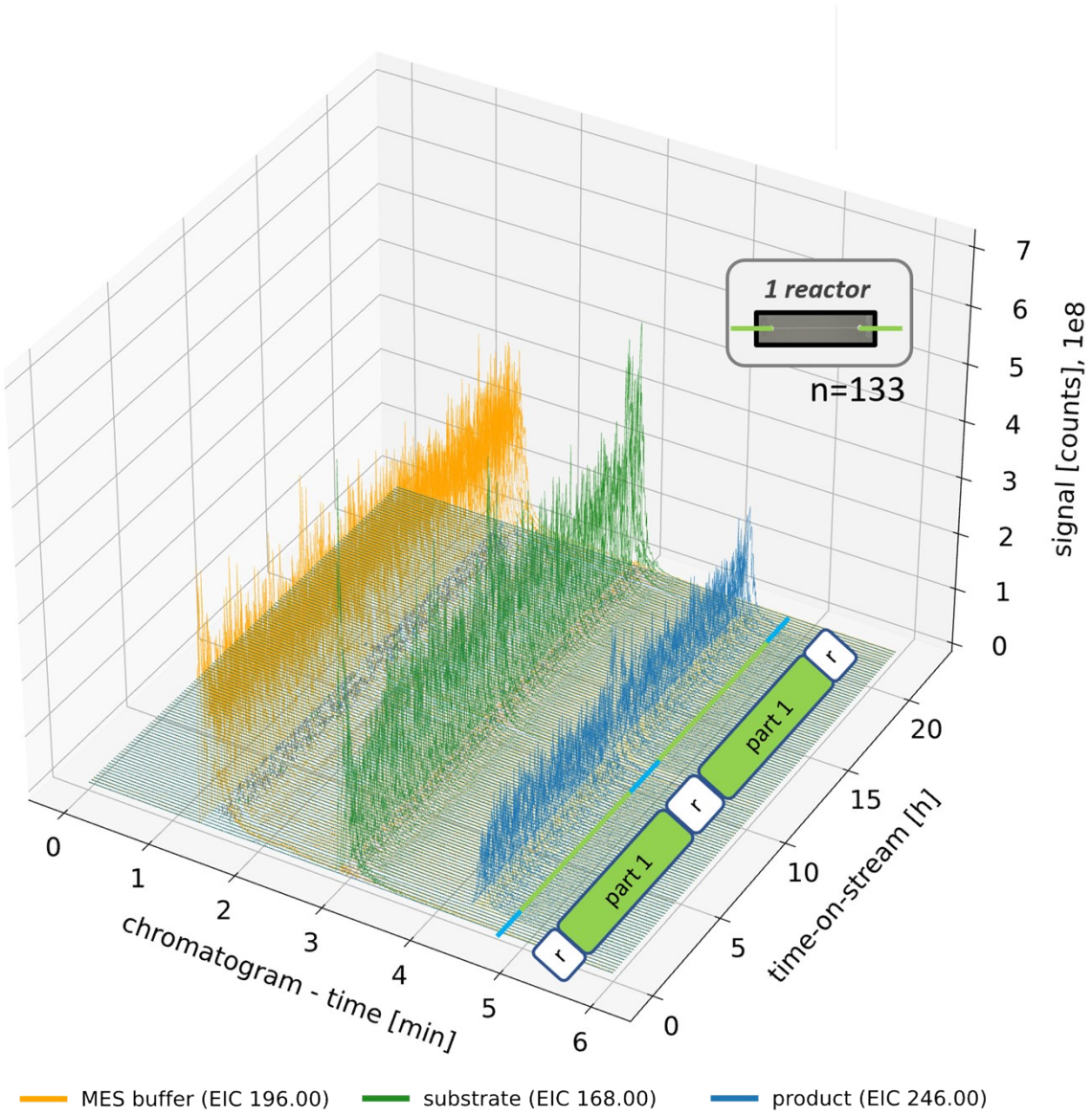

Fig. S25 Monitoring a single µreactor run using a packed-bed reactor with on ProntoSil immobilized *Ci*VHPOHalo enzyme and constant sample feed utilizing a complexer pre-programmed sequence. At the beginning, in the middle as well as at the end of the reactor run the reactor position were switched by the selector valves to a blank capillary to investigate the pure pump or sample feed (n=133, approx. approx. 22 h, samping each 10 min; EIC only for one brominated product **2** isotope shown). The rct. mix. 1 was used as listed in Table S1. A detailed evaluation of each reactor run is shown below in Fig. S26. For this run none of the discussed byproducts **S2-S5** were observable. Reactor: packed with CiVHPOHalo on ProntoSil particles (ø 5 µm, loading f = 7.47 µg·mg^{-1}), rct. pump: 0.2 µl·min^{-1} 50 mM MES-buffer (residence time approx. 40 s, flushing sample loop with 2 µl·min^{-1} for 3 min at start; dilution: 2 µl·min^{-1} MeCN:H_2O, 60:40 vol% with 50 mM MES as sample); Analysis: Zorbax Eclipse Plus (C18, 4.6x100 mm, 3.5 µm, Agilent), 600 µl·min^{-1} MeCN:H_2O (70:30 vol% with 0.1% FA, 52 bar at pump, 2 µl injection volume. "r": blank sample, "R1": reactor run.

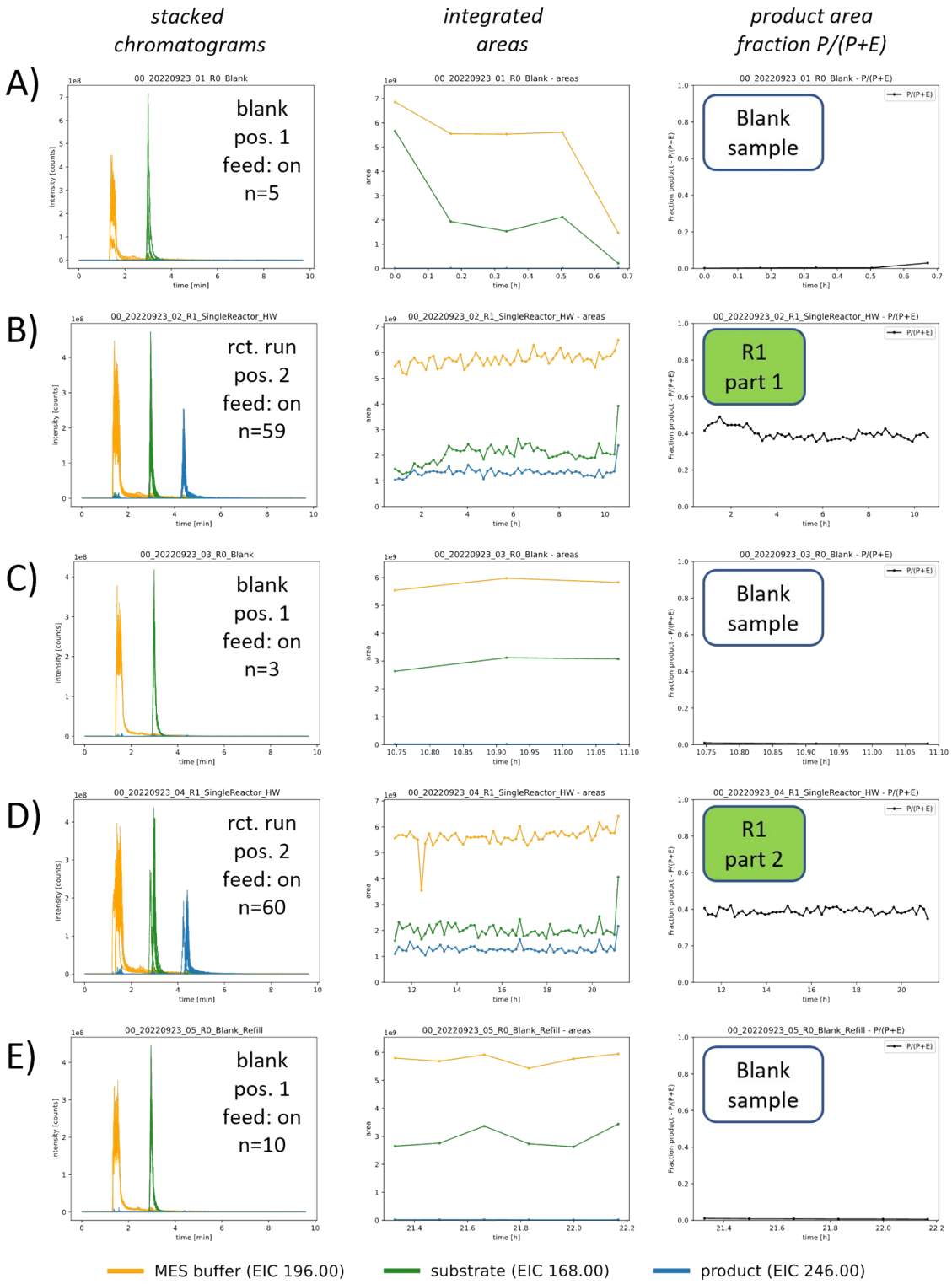

Fig. S26 Visualisation of all respective subparts of the sequence of the combined single µreactor packed-bed µreactor run as shown in before in Fig. S25. For acquiring the blank measurements, the µreactor selection valve was switched onto a blank capillary during the run bypassing the reactor. capillary (n=133, approx. approx. 22 h, sampling each 10 min; only one brominated product **2** isotope considered for visualization). The rct. mix. 1 was used as listed in Table S1. For this run none of the discussed byproducts **S2-S5** were observable. **A)** washing/blank, pos. 1, **B)** reactor run part 1, pos. 2, **C)** washing/blank, pos. 1, **D)** reactor run part 2, pos. 2 **E)** washing/blank, pos. 1; Reactor: packed with *Ci*VHPOHalo on ProntoSil particles (ø 5 µm, loading f = 7.47 µg·mg^{-1}), rct. pump: 0.2 µl·min^{-1} 50 mM MES-buffer (residence time approx. 40 s, flushing sample loop with 2 µl·min^{-1} for 3 min at start; dilution: 2 µl·min^{-1} MeCN:H_2O, 60:40 vol% with 50 mM MES as sample); Analysis: Zorbax Eclipse Plus (C18, 4.6x100 mm, 3.5 µm, Agilent), 600 µl·min^{-1} MeCN:H_2O (70:30 vol% with 0.1% FA, 52 bar at pump, 2 µl injection volume.

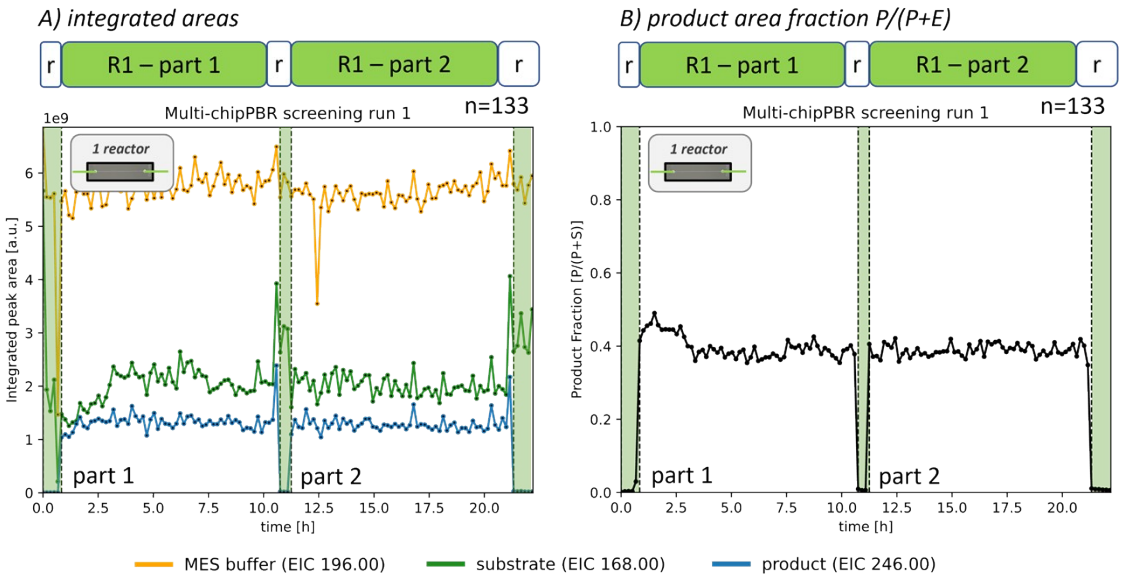

Fig. S27 Evaluation of the integrated peak area of the packed-bed µreactor run, with more complex sequence, adding blank acquisitions during the run, by the selector valves to a blank capillary (n=133, approx. approx. 22 h, samping each 10 min; only one brominated product **2** isotope considered for visualization and comparison). The rct. mix. 1 was used as listed in Table S1. For this run none of the discussed byproducts **S2**-**S5** were observable. **A)** integrated peak areas of the buffer, reactant **1**, and product **2** EIC-traces. **B)** Plot showing the product **2** area fraction. Reactor: packed with *Ci*VHPOHalo on ProntoSil particles (ø 5 µm, loading f = 7.47 µg·mg^{-1}), rct. pump: 0.2 µl·min^{-1} 50 mM MES-buffer (residence time approx. 40 s, flushing sample loop with 2 µl·min^{-1} for 3 min at start; dilution: 2 µl·min^{-1} MeCN:H_2O, 60:40 vol% with 50 mM MES as sample); Analysis: Zorbax Eclipse Plus (C18, 4.6x100 mm, 3.5 µm, Agilent), 600 µl·min^{-1} MeCN:H_2O (70:30 vol% with 0.1% FA, 52 bar at pump, 2 µl injection volume. "r": blank sample, "R1": reactor run.

- *Multi-reactor screening run with sample variation:*

The integration of an autosampler before the µreactor selector valves, significantly increased the setup flexibility during individual runs (instead of using the constant sample feed from the sample valve as before), as multiple different reaction samples could be tested sequentially on similar or different µreactor positions with different packed-bed µreactors (as shown in Fig. S28 below).

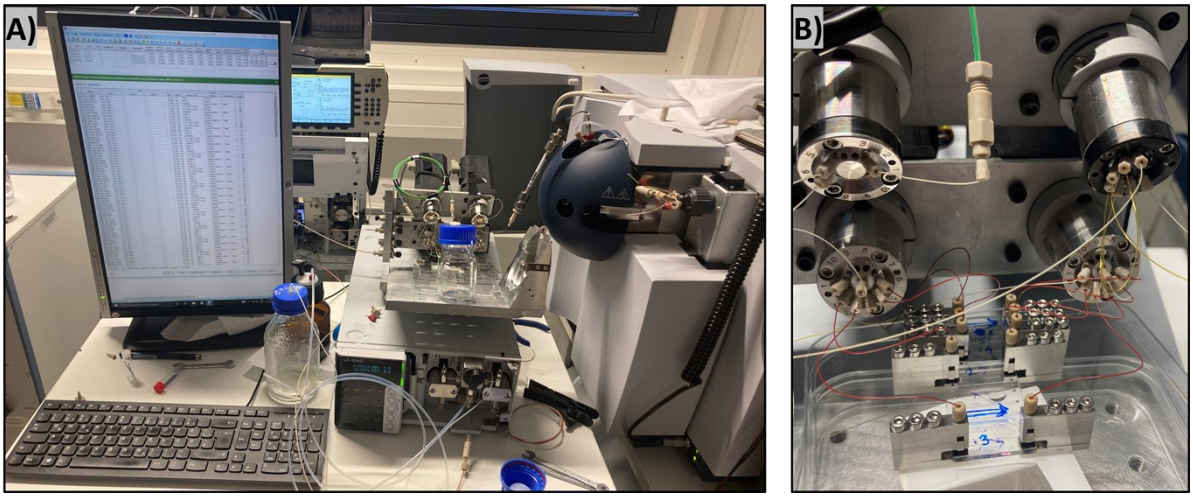

Fig. S28 A) Instrumental setup for multi-reactor screening in front of the mass spectrometer. **B)** Connection of multiple continuous microreactors using custom built clamps connected to the µreactor channels. Furthermore, the respective selector valves are shown for actively selecting the respective reactors.

This functionality can be used for automated screening approaches for reaction optimization, as highlighted in the following automated run. Here, multiple different packed-bed µreactors were monitoring sequentially for multiple hours, each with a different sample feed (the different tested sample compositions can be found in section S4.3 at Table S1). The respective sequence used is depicted in Fig. S29 and shortly discussed below (the method structure approach had to be structured slightly different too, after autosampler coupling). Similarly, all resulting chromatograms are depicted together in a waterfall chromatogram in Fig. S30 and all respective subparts and integrated areas as well as product fractions are discussed afterward.

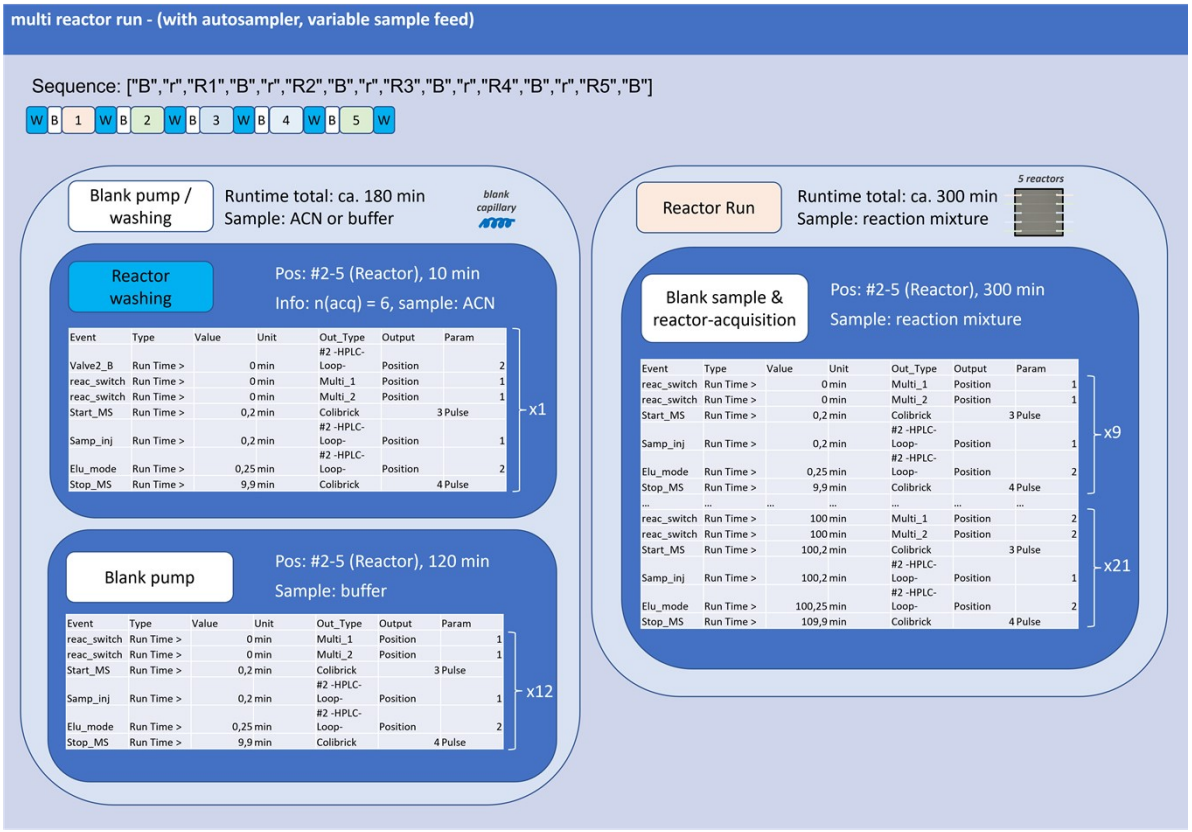

Fig. S29 Sequence performed for testing different reactors with different samples. Each reactor was monitored for 300 min, performing LC-MS injections each 10 min. Furthermore, multiple blanks (B) and sample blanks (r) were acquired before to evaluate first the pump feed and then the sample feed after the sample feed was integrated. In addition, the reactor line was washed or equilibrated by flushing buffer onto the reactor and measuring cleaning process by monitoring the pump feed (w, n=6). Shown are the utilized event tables as defined in the "Clarity" software for each method/function block as described in Fig. S11. "w"/"B": washing / blank pump, "r": blank sample, "R1": reactor run.

The run started at the blank capillary position starting with a washing step to flush the line while the blank capillary was selected as reactor position (**„washing"**, **„w"**, pos. 1, n=6, injecting CAN through the autosampler). Thereafter, further blank measurements of the pure pump feedback were measured as baseline (**„Blank Sample/Pump"**, **„B"**, pos. 1, n=12, injecting buffer).

Then, the reactor acquisition method was started, and the first sample was injected by the autosampler (40 µl). Since the autosampler was located before the µreactor positions it took some time, till the sample was transferring through the µreactor selection valves, the blank capillary and finally the sample loop of the analytical section (approx. 60-80 min, compare Fig. S30). Due to that, multiple additional blank measurements were acquired (**„Blank"**, **„B"**, pos. 1, n=9), to observe when the autosampler injected sample plug reached a plateau and thereafter, the selector valves were switched automatically onto the first packed-bed µreactor (**„Reactor 1"**, **„R1"***;* pos. 2, Fig. S31 A. These sample blank measurements could also be used as a reactant signal baseline before switching to the reactor, to later calculate the sample conversion. Now, the µreactor was monitored until the plateau of the injected sample was decreasing again (n=16, approx. 160 min). After the run another washing step was conducted as well as the blank until the next sample was injected. This duty cycle was repeated for each µreactor position,

and all sample mixtures tested (**„Reactor 2-5”**, **„R2-5”***;* pos. 3-6) with a subsequent final washing step (**„washing”**, **„w”**, pos. 1, n=6).

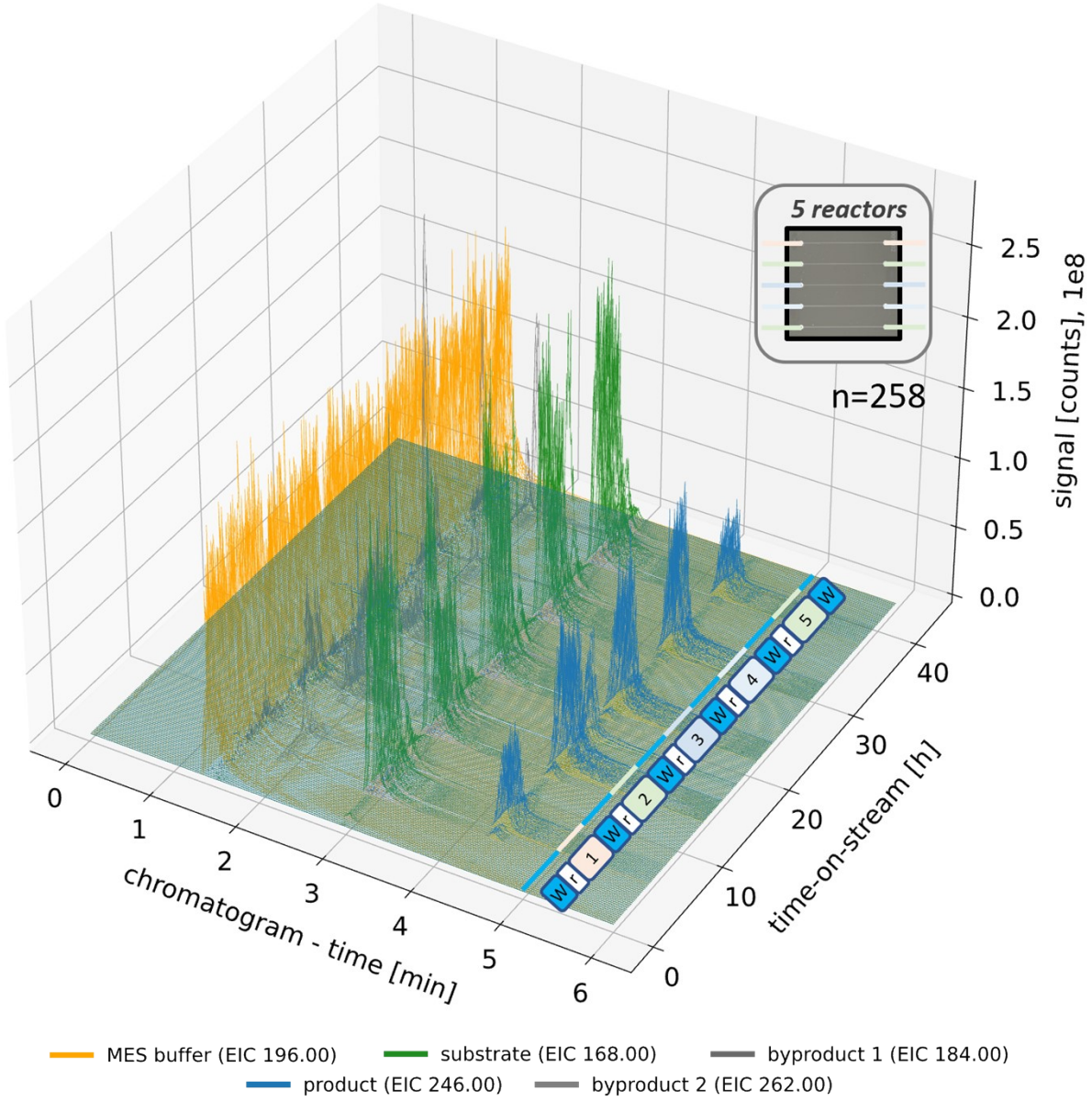

Fig. S30 Waterfall diagram of all acquired chromatograms of the automated sequential approach monitoring five connected packed-bed µreactors (n=258, approx. 43 h, sampling each 10 min; EIC only for one brominated product **2** isotope shown). Each reactor position selected (pos. 2-6) were sampled by the autosampler with a varying reaction mixture (40 µl sample, each reactor run n=16, approx. 160 min; The rct. mix. 1-4 were used as listed in Table S1. For comparison was the last µreactor channel only half-packed. Before each reactor run, multiple blank acquisitions were acquired for pump or sample feed observation and likewise a washing step was conducted after each reactor run (pos 1, blank capillary). Reactor: packed with *Ci*VHPOHalo on ProntoSil particles (ø 5 µm, loading f = 20.6 µg·mg^{-1}), rct. pump: 0.2 µl·min^{-1} 50 mM MES- buffer (residence time approx. 40 s, no dilution); Analysis: Zorbax Eclipse Plus (C18, 4.6x100 mm, 3.5 µm, Agilent), 600 µl·min^{-1} MeCN:H_2O (70:30 vol% with 0.1% FA, 51 bar at pump, 0.2 µl injection volume. “w”/“B”: washing / blank pump, “r”: blank sample, “R1”: reactor run.

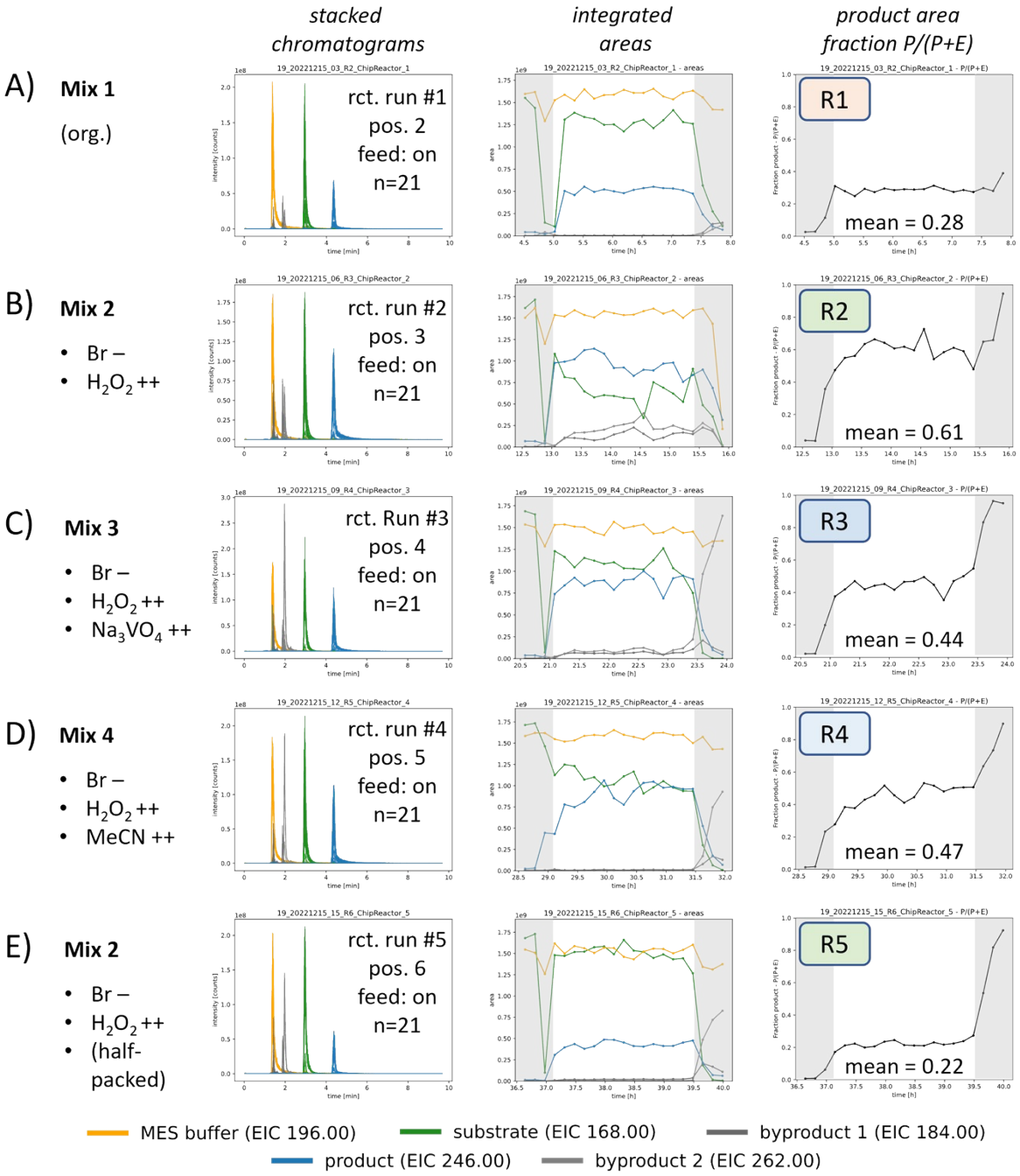

Fig. S31 Insight to the different reactor runs of the fully automated multi-reactor run with 4 different samples tested on five different reactor positions packed with the same on silica immobilized enzyme (n=258, approx. 43 h, sampling each 10 min; only one brominated product **2** isotope considered for visualization). For comparison is the last µreactor (E) only half-packed. The rct. mix. 1-4 were used as listed in Table S1. Sample mixture 2 (B) showed the highest conversion and product **2** fraction, however also the highest amount of observed byproduct **S2**-**S5** during the reactor run. Reactor: packed with *Ci*VHPOHalo on ProntoSil particles (ø 5 µm, loading f = 20.6 µg·mg^{-1}), rct. pump: 0.2 µl·min^{-1} 50 mM MES- buffer (residence time approx. 40 s, no dilution); Analysis: Zorbax Eclipse Plus (C18, 4.6x100 mm, 3.5 µm, Agilent), 600 µl·min^{-1} MeCN:H_2O (70:30 vol% with 0.1% FA, 51 bar at pump, 0.2 µl injection volume.

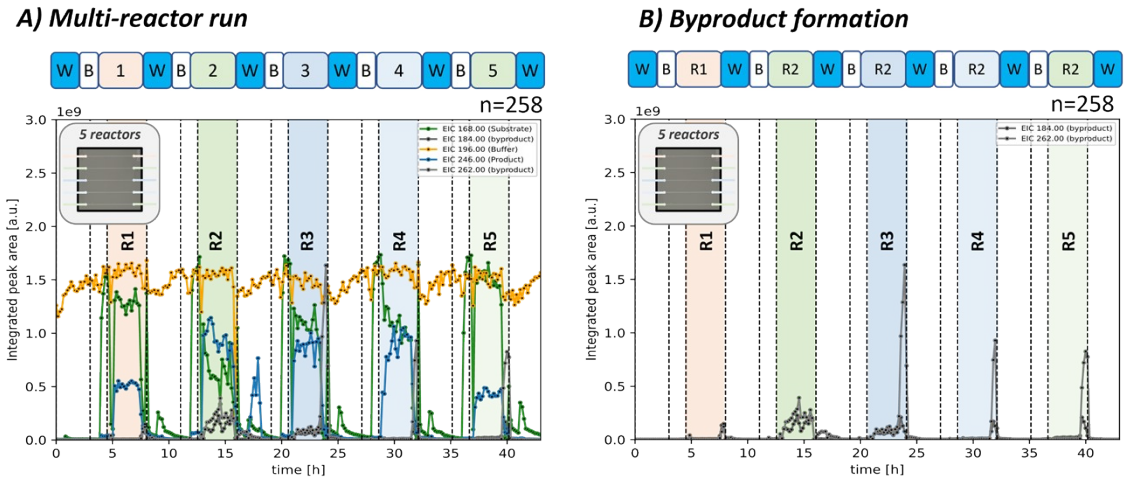

Fig. S32 Automated sequential sample screening approach for monitoring five connected packed-bed µreactors (n=258, approx. 43 h, sampling each 10 min; only one brominated product **2** isotope considered for visualization). Each reactor position selected (pos 2-6) were sampled by the autosampler with a different reaction mixture (40 µl sample, each reactor run n=16, approx. 160 min, pos. 2-6); The rct. mix. 1-4 were used as listed in Table S1. Before each reactor run, multiple blank acquisitions were acquired for pump or sample feed observation and likewise a washing step was conducted after each reactor run (pos. 1, blank capillary). **A)** Integrated peak areas, using only the EIC traces of the buffer, reactant **1** and product **2**. **B)** Integrated areas of the EIC traces for byproduct formation (as discussed in section 4.3). Reactor: packed with *Ct*VHPOHalo on ProntoSil particles (Ø 5 µm, loading f = 20.6 µg·mg^{-1}), rct. pump: 0.2 µl·min^{-1} 50 mM MES- buffer (residence time approx. 40 s, no dilution); Analysis: Zorbax Eclipse Plus (C18, 4.6x100 mm, 3.5 µm, Agilent), 600 µl·min^{-1} MeCN:H_2O (70:30 vol% with 0.1% FA, 51 bar at pump, 0.2 µl injection volume. “w”/“B”: washing / blank pump, “r”: blank sample, “R1”: reactor run.

5.3. Part_3 - ChipLC setup integration for solvent reduction

- *ChipHPLC - Injection principle*

As previously mentioned, several applications of the presented chipHPLC can be found in literature[2–4,6,9]. The simplified injection principle employed in this project is based on a previous joint publication.[7] It is utilized here as a compact modular chipHPLC unit, offering an alternative to conventional columns for achieving solvent reduction and fast separations. The injection principle consists of two modes, the elution and injection mode, which are controlled by an external valve, which influences the direction of the direction and velocities of the streams within the chipHPLC (see Fig. S33 A1-B1).

During the elution mode, the full eluent flow is guided to the chip through the ”eluent” channel entry. Inside the chip, the eluent stream is split into two directions at the injection cross. While one part of the flow is directed onto the integrated chip-column as the eluent, the remaining portion is guided to the ”waste” outlet channel. To control this flow split and regulate the eluent flow on the column, a restriction capillary was added to the waste channel (w1, ID=25 µm, l=22 cm). Additionally, the pressure was monitored using an external pressure sensor (p). In this mode, it was also possible to refill the sample loop connected to the valve. This could be achieved either by coupling it to the constant reactor effluent of the previously presented µreactor setup as the sample feed or by using an external syringe during testing.

When switching to the injection mode, an additional flow split is opened directly after the eluent pump. This flow split is determined by the length and inner diameters of the connected capillaries and is adjusted to achieve a flow split ratio of 1:1 (v/v), as confirmed by the resulting pressures. In this mode, one part of the flow is directed toward the on-chip injection cross with a reduced volume stream due to the flow split. The other part flows through the valve, passes through the loaded sample loop, and enters the chip through the ”sample” inlet, finally reaching the integrated injection cross. During this so-called ”pinched” injection process, a fraction of the sample plug accumulates at the column cross within the

injection cross. It can be subsequently eluted by switching back to the eluent mode with an increased eluent flow present. By reducing of the eluent flow rate and using an alternative restriction length at the waste outlet during the injection mode to a lower pressure situation in the injection cross (w2<w1; ID=100 µm, l=20 cm), the amount of loaded sample can be controlled, effectively minimizing extensive pre-elution of the sample plug before switching back the elution mode.

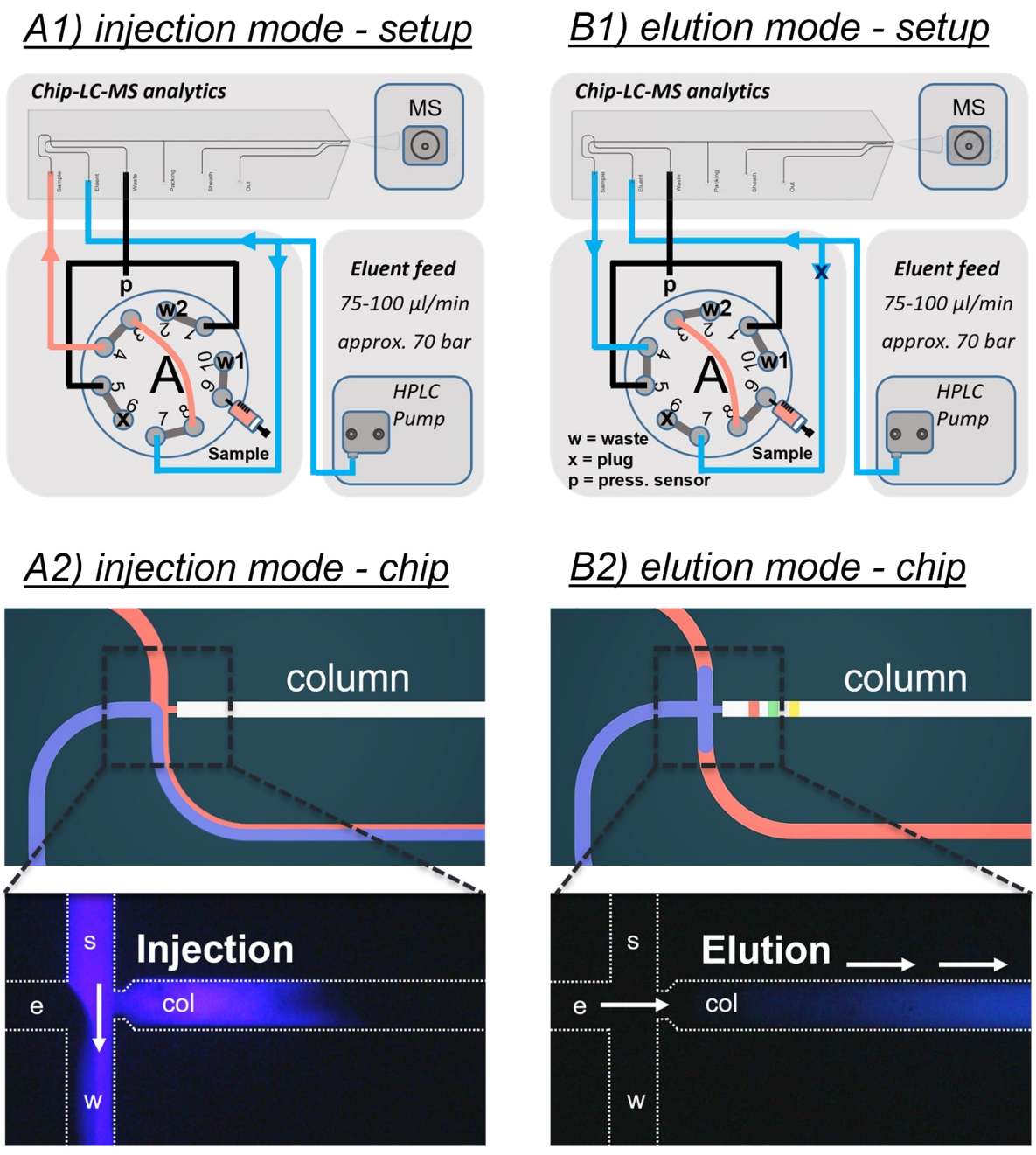

Fig. S33 A) Visualization of the injection principle by injecting a fluorescent dye as sample (Coumarin 120, 100 µg/ml). Here, the sample was illuminated and observed in the on-chip injection cross through an epi-fluorescence microscope (channels: s=sample, e=eluent, w=waste, c=column). **A)** During the injection mode the sample is directed to the injection cross, with a fraction accumulating at the column head; **B)** During the elution mode, the sample can be eluted along the separation column with increased velocity.

To investigate the injection principle and visualize flow dynamics in the chipHPLC setup, a fluorescent dye (Coumarin 120, 100 µg/ml) was injected as sample and observed within the on-chip injection cross using an epi-fluorescence microscope, as depicted in Fig. S33 A2-B2. Afterward, the sample was

illuminated by a high-pressure mercury vapor lamp to investigate the stability of the injection principle for different eluent compositions, injection times and flow rates tested. For that purpose, an excitation bandpass filter (350/50 nm) was initially employed. The light was then guided through a long-pass filter (> 390 nm) and finally a dichroic filter (380 nm) before observation. During the verification of the injection principle, particular focus was set on the formation of the pinch flow and subsequent sample plug formation at the column head during the injection mode, as well as the overall injection of the sample plug when switching back to the elution mode. In addition, the injection principle was optimized toward achieving minimal sample plug pre-elution during the injection mode.

For that purpose, different flow rates (25-100 µl/min) and compositions were tested (50:50 – 90:10, ACN:H_2O, v/v). The results demonstrated successful injection principles and satisfactory flow behaviour, as shown in Table S2, along with further evaluation parameters. It should be noted that slower flow rates allow more flexibility in the timing of valve switching between the injection and elution modes to transfer the sample plug from the injection cross, as it allows for longer periods of loop exhaustion. However, thanks to the automation of the valving duty cycle, shorter injection times are also feasible.

Table S2 Tested chipHPLC eluent parameters for different eluent compositions and flow rate compositions, ensuring a stable injection principle. The time required to exhaust the sample loop is also provided, as it is relevant for achieving optimal transfer timing during injection. The column dead time and lateral flow rate were approximated using the injected coumarin sample as dead time marker due to its low retention on C18 stationary material.

S.No	eluent composition [ACN:H_2O]	flow rate [µL/min]	arrival time[s]	loop exh. [s]	column dead time[s]	lateral flow rate [mm/s]
1	50/50	25	1	20	61	0.57
2	50/50	50	1	5	36	0.97
3	50/50	75	1	3	25	1.40
4	70/30	25	1	30	54	0.65
5	70/30	50	1	8	32	1.09
6	70/30	75	1	3	23	1.52
7	70/30	100	1	2	14	2.50
8	90/10	25	1	30	46	0.76
9	90/10	50	1	12	26	1.35
10	90/10	75	1	5	20	1.75
11	90/10	100	1	3	16	2.19
12	90/10	150	0.5	2	11	3.18

- *ChipLC separation optimization – batch reaction*

As an additional feature for solvent reduction and achieving fast, but efficient separations, a chipLC module was integrated into the analytical section of the setup. Further information on the setup can be found in section S2.2. For initial evaluation, the chipLC setup was tested by injecting a batch sample with free enzyme (3.7 µM in sample before dilution) added through a syringe as sample feed. Here the focus was set on the optimization of the separation parameters and overall performance. The achieved separation is depicted in Fig. S34 A-B (n=10), showing the similar components as before without any byproduct formation. Here the retention time of the buffer was t_R = 28.8 ± 1.21 s (± 4.20%), the reactant **1** t_R = 49.0 ± 0.63 s (± 1.30%) and for the product **2** t_R = 70.1 ± 0.61 s (± 0.88%). Furthermore, the detected pressure data of the analogous detection channels first at the elution pump and at the external pressure sensor at the chip outlet before the restriction capillaries (thus, referencing the pressure at the injection cross) is plotted in Fig. S34 C. Here, the low-pressure situation during the injection mode is visualized, enabling the pinched injection without any pre-elution effects of the sample plug onto the column, before switching back to the elution mode. In addition, for all acquisitions at Fig. S34 D. The data shows high pressure stability and fast pressure buildup after the low-pressure injection situation, which is necessary to achieve a sufficient separation performance and reduction of peak-broadening effects. Generally, when looking at the chromatogram (Fig. S34 A), the separation time could be decreased below 2 min, which can result in an increased acquisition frequency of the

automated setup duty cycle. However, while the pressure buildup after the injection reaching around 80% of the initial value after only a few seconds, it requires approximately 5 min to completely recover, which is the reason we set the injection duty cycle time to that time. In future works this could be lowered by further adapting the internal volumes, variate the restriction capillaries and pump hardware changes.

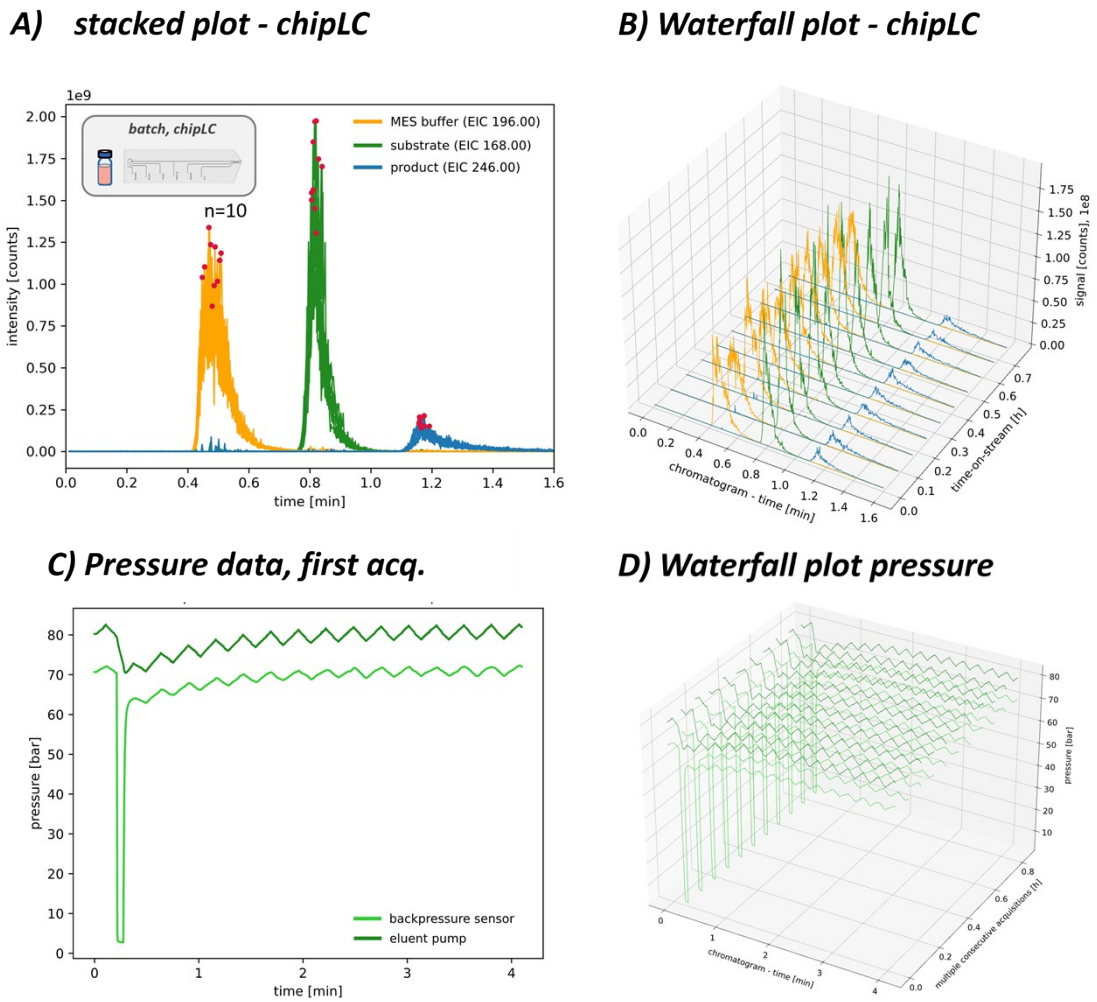

Fig. S34 ChipHPLC runs for evaluating reproducibility and initial separation optimization. The reaction was performed in batch for this run and sampled into the injection loop through a syringe. **A)** Stacked plot of all chromatograms (n=10, approx. 0.8 h, sampling each 4 min; only one brominated product **2** isotope considered for visualization), visualizing the respective peak maxima used for the calculated retention times with red dots. **B)** All acquired chromatograms plotted in a waterfall diagram; **C)** Visualisation of the pressure data for one individual run. Here the pressure at the eluent pump as well as the pressure at the chip outlet was measured. A pressure drop can be observed during the injection principle, as required during the injection mode to avoid pre-elution of the sample plug on the column head. When switching back to the elution mode, the pressure rises back. **D)** Waterfall diagram of the pressure data of all acquired runs; Reactor: 1:10 diluted homogeneous batch reaction sampled into the sample loop continuously using a syringe pump (rct. mix. 1, see Table S1 with 3.7 µM homogeneous free enzyme added); Analysis: Xbridge particles 35 mm column length (C18, ∅ 2.5 µm, Agilent), eluent flow: 75 µl·min^{-1} MeCN:H_2O (50:50 vol% with 0.1% FA,), during elution mode: 80 bar at pump, 71 bar at chip, 5 µl injection volume, 7 s injection time.

- *ChipLC – application - µreactor coupling*

Similar as the presented above with the conventional C18-column, the chipLC was then coupled to a packed-bed µreactor as sample feed. For that purpose, an older already used µreactor was used, which resulted in significantly reduced conversion performance and fast enzyme deactivation observed However, since the immobilized enzyme efficiency was already presented before, the focus was set here on the stability of the coupling of the two setups and resulting separation performance (n=25,

approx. 2 h). In addition, by variation of the injection time and thus different sample loading at the injection cross, even better separation efficiency could be achieved as shown in Fig. S35 A. Here the retention time of the buffer was t_R = 21.3 ± 0.46 s (± 2.19%), the reactant **1** t_R = 50.8 ± 0.60 s (± 1.17%) and for the product **2** t_R = 78.5 ± 0.94 s (± 1.20%). In the future this could be further tested to be fully implemented in further complex multi-reactor screening experiments as presented here before with conventional separation columns, to benefit from the fast separation at low solvent consumption.

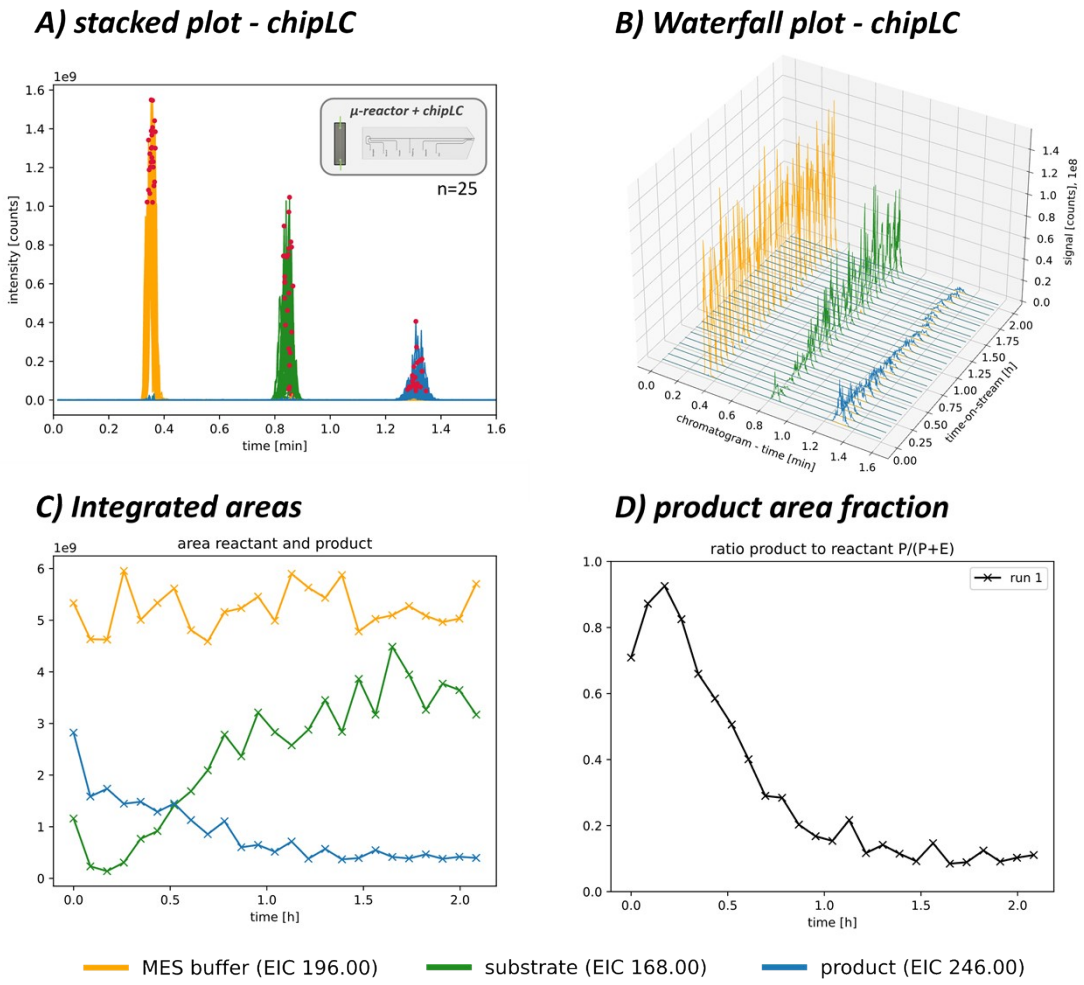

Fig. S35 chipHPLC run for the model reaction coupled to an already used packed-bed µreactor. **A)** Stacked plot of all chromatograms (n=25, approx. 2 h, sampling each 5 min; only one brominated product **2** isotope considered for visualization), visualizing the respective peak maxima used for the calculated retention times with red dots. **B)** All acquired chromatograms plotted in a waterfall diagram; **C)** Course of the integrated areas for the reactant **1**, buffer and product **2** peak. **D)** Plot showing the course product **2** area fraction; Reactor: packed with *Ci*VHPOHalo on ProntoSil particles (ø 5 µm), rct. mix. 1, (see Table S1), rct. pump: 0.2 µl·min^{-1} 50 mM MES (residence time approx. 40 s, flushing sample loop with 2 µl·min^{-1} for 3 min at start, dilution: 2 µl·min^{-1} MeCN:H_2O, 60:40 vol% with 50 mM MES as sample); Analysis: Xbridge particles 35 mm column length (C18, ø 2.5 µm, Agilent), eluent flow: 75 µl·min^{-1} MeCN:H_2O (50:50 vol% with 0.1% FA,), during elution mode: 72 bar at pump, 70 bar at chip, 5 µl injection volume, 4 s injection time.

- *ChipLC – system stability evaluation – µreactor coupling*

Just to further evaluate and highlight the automated chipLC long-term system stability the previous experiment with the already deactivated prior packed-bed µreactor chip was conducted further. The resulting stability of the retention times in combination with the pressure curves for all acquired measurements are shown in Fig. S36 (n=216 chromatograms, approx. 18 h, sampling each 5 min). Here the retention time of the buffer was t_R = 21.7 ± 0.53 s (± 2.43%), the reactant **1** t_R = 50.8 ± 0.92 s (± 1.81%) and for the product **2** t_R = 78.0± 1.64 s (± 2.10%). As mentioned before

additional runs should be conducted in the future in more complex µreactor runs to benefit from the fast separation at low solvent consumption. Furthermore, due to the high degree of automation also further data processing and feedback loop based methods could be implemented in the future.

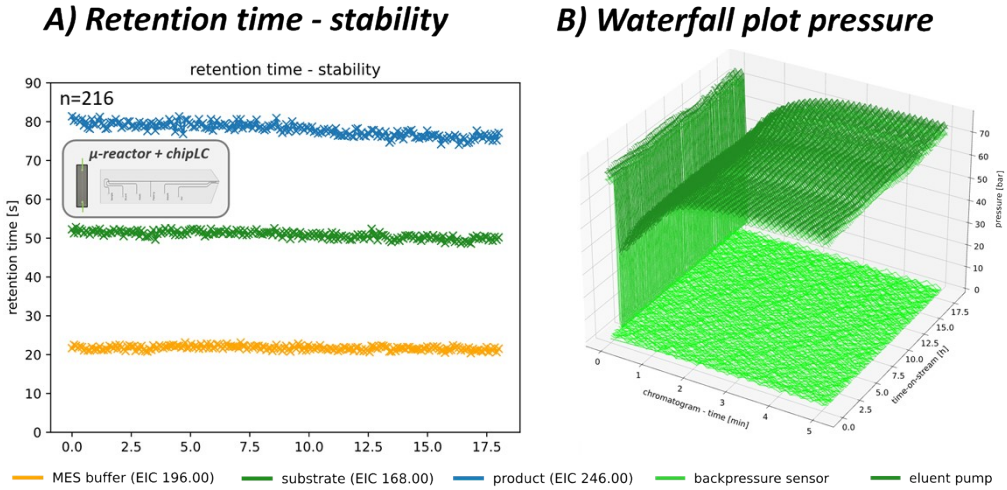

Fig. S36 long-term-stability test visualization the retention time consistency of an additional chipHPLC run using an already used packed-bed µreactor. **A)** Course of the retention times during the long-term stability test, observing each acquired chromatogram (n=216, approx. 18 h, sampling each 5 min; EIC of only one brominated product **2** isotope considered); **B)** Waterfall diagram of the pressure data of all acquired runs; Reactor: packed with *Ci*VHPOHalo on ProntoSil particles (Ø 5 µm), rct. mix. 1 (see Table S1), rct. pump: 0.2 µl·min^{-1} 50 mM MES (residence time approx. 40 s, flushing sample loop with 2 µl·min^{-1} for 3 min at start, dilution: 2 µl·min^{-1} MeCN:H_2O, 60:40 vol% with 50 mM MES as sample); Analysis: Xbridge particles 35 mm column length (C18, Ø 2.5 µm, Agilent), eluent flow: 75 µl·min^{-1} MeCN:H_2O (50:50 vol% with 0.1% FA,), during elution mode: 72 bar at pump, 70 bar at chip, 5 µl injection volume, 4 s injection time.

- *ChipLC – simple variant:*

During the development and optimization of the chipLC setup, an alternative simplified version was initially tested and evaluated. In this variant, an additional external injection valve (equipped with an integrated 5 nl loop; Nanovolume valve, Cheminert, Vici Valco) was used instead of the later implemented on-chip integrated injection cross. With this approach, the full flow from the eluent pump (capillary pump G1376A, Agilent) was directly connected to the chipLC (instead of using an eluent flow split in the injection cross). The chipLC system was then similarly coupled to the MS-inlet using a grinded nanospray-emitter integrated at the chip. The advantage of this approach was that the setup could be operated with a significantly lower eluent flow rate of 0.75 µl/min, which was comparable to the flow rate used in the reactor. It was generally possible to separate the reactant **1** and product **2** peak with approach (see Fig. S37). However, to achieve sufficient separation, an increase of the aqueous fraction was required (up to 60%) which resulted in unstable nanospray performance and relatively high noise levels. Additionally, due to the external sampling strategy, increased peak broadening could be observed. Consequently, despite the remarkably low solvent consumption, the previously presented chipHPLC approach is preferred (which utilizes a higher flow rate of approx. 75-100 µl/min).

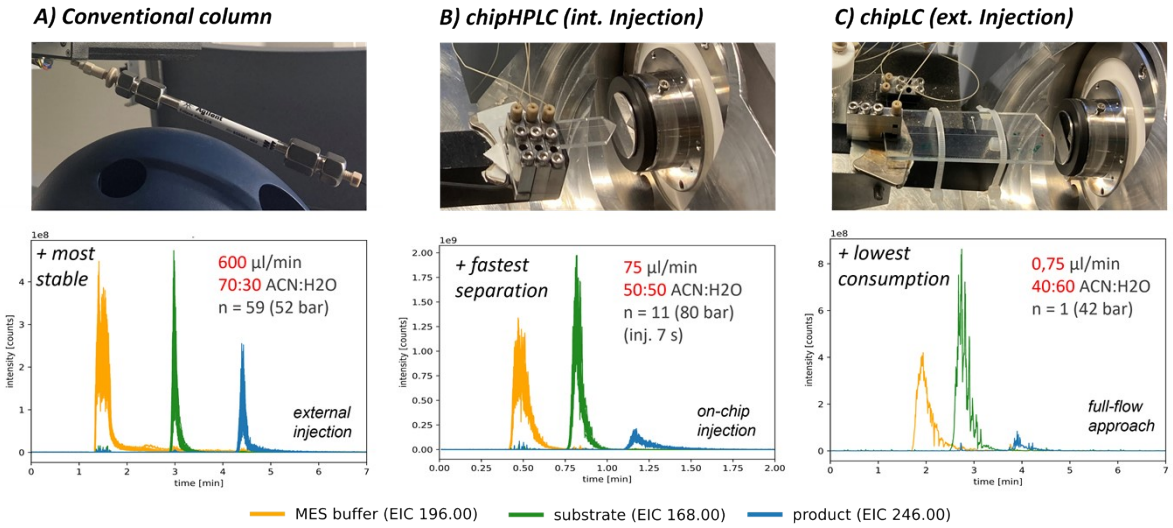

Fig. S37 Comparison of the separation of the different LC-systems tested (either conventional or chipLC; EIC of only one brominated product **2** isotope shown); **A)** Conventional C18-column, stationary phase: Zorbax Eclipse Plus (C18, 4.6x100 mm, 3.5 µm, Agilent); mobile phase: 600 µl/min, 70:30 MeCN:H_2O (v/v); **B)** Sophisticated chipHPLC approach with integrated injection cross. Here run shown with multiple injections of the same biotransformation performed in batch, stationary phase: XBridge (C18, 2.5 µm, Waters); mobile phase: 75-100 µl/min, 50:50 MeCN:H_2O (v/v); **C)** chipLC with full flow approach with external injection through valving, stationary phase: Exsil Pure C18MS (3 µm, Dr Maisch GmbH), mobile phase: 0.75 µl/min, 40:60 MeCN:H_2O (v/v).

8. References

[1] S. K. Piendl, T. Schönfelder, M. Polack, L. Weigelt, T. van der Zwaag, T. Teutenberg, E. Beckert, D. Belder, *Lab. Chip* **2021**, *21*, 2614–2624.
[2] C. Lotter, J. J. Heiland, V. Stein, M. Klimkait, M. Queisser, D. Belder, *Anal. Chem.* **2016**, *88*, 7481–7486.
[3] J. J. Heiland, C. Lotter, V. Stein, L. Mauritz, D. Belder, *Anal. Chem.* **2017**, *89*, 3266–3271.
[4] J. J. Heiland, D. Geissler, S. K. Piendl, R. Warias, D. Belder, *Anal. Chem.* **2019**, *91*, 6134–6140.
[5] S. K. Piendl, C.-R. Raddatz, N. T. Hartner, C. Thoben, R. Warias, S. Zimmermann, D. Belder, *Anal. Chem.* **2019**, *91*, 7613–7620.
[6] C. Lotter, J. J. Heiland, S. Thurmann, L. Mauritz, D. Belder, *Anal. Chem.* **2016**, *88*, 2856–2863.
[7] K. Svensson, C. Weise, H. Westphal, S. Södergren, D. Belder, K. Hjort, *Sens. Actuators B Chem.* **2023**, *385*, 133732.
[8] S. Thurmann, A. Dittmar, D. Belder, *J. Chromatogr. A* **2014**, *1340*, 59–67.
[9] S. Thurmann, L. Mauritz, C. Heck, D. Belder, *J. Chromatogr. A* **2014**, *1370*, 33–39.
[10] S. Thurmann, C. Lotter, J. J. Heiland, B. Chankvetadze, D. Belder, *Anal. Chem.* **2015**, *87*, 5568–5576.
[11] H. Westphal, R. Warias, H. Becker, M. Spanka, D. Ragno, R. Gläser, C. Schneider, A. Massi, D. Belder, *ChemCatChem* **2021**, *13*, 5089–5096.
[12] H. Westphal, R. Warias, C. Weise, D. Ragno, H. Becker, M. Spanka, A. Massi, R. Gläser, C. Schneider, D. Belder, *React. Chem. Eng.* **2022**, *7*, 1936–1944.
[13] L. F. Vistain, M. W. Rotz, R. Rathore, A. T. Preslar, T. J. Meade, *Chem. Commun.* **2016**, *52*, 160–163.
[14] Y. Sun, F. Kunc, V. Balhara, B. Coleman, O. Kodra, M. Raza, M. Chen, A. Brinkmann, G. P. Lopinski, L. J. Johnston, *Nanoscale Adv.* **2019**, *1*, 1598–1607.
[15] D. R. Morris, L. P. Hager, *J. Biol. Chem.* **1966**, *241*, 1763–1768.
[16] C. J. Seel, A. Králík, M. Hacker, A. Frank, B. König, T. Gulder, *ChemCatChem* **2018**, *10*, 3960–3963.
[17] R. Renirie, C. Pierlot, J.-M. Aubry, A. F. Hartog, H. E. Schoemaker, P. L. Alsters, R. Wever, *Adv. Synth. Catal.* **2003**, *345*, 849–858.
[18] J. K. Howard, K. J. Rihak, A. C. Bissember, J. A. Smith, *Chem. – Asian J.* **2016**, *11*, 155–167.